DISSERTATIONES
GEOLOGICAE
UNIVERSITATIS
TARTUENSIS
54

RAUL PAAT

Groundwater and surface water interactions in peatlands: Hydrogeological insights from Estonian mires

DISSERTATIONES GEOLOGICAE UNIVERSITATIS TARTUENSIS
54

RAUL PAAT

Groundwater and surface water interactions in peatlands: Hydrogeological insights from Estonian mires

UNIVERSITY OF TARTU
Press
1632

Department of Geology, Institute of Ecology and Earth Sciences, Faculty of Science and Technology, University of Tartu, Estonia.

This dissertation is accepted for the commencement of the degree of Doctor of Philosophy in Geology at the University of Tartu on the 29th of August 2024 by the Scientific Council of the Institute of Ecology and Earth Sciences, University of Tartu.

Supervisors: Argo Jõeleht, Department of Geology, University of Tartu, Estonia
Marko Kohv, Department of Geology, University of Tartu, Estonia

Opponent: prof. Jonathan S. Price, University of Waterloo, Canada

This thesis will be defended at the University of Tartu, Estonia, Chemicum (Ravila 14A), room 1019, on the 3rd of October 2024 at 12:15

Publication of this thesis was granted by the Institute of Ecology and Earth Sciences, University of Tartu

ISSN 1406-2658 (print)
ISBN 978-9916-27-645-7 (print)
ISSN 2806-2310 (pdf)
ISBN 978-9916-27-646-4 (pdf)

University of Tartu Press
www.tyk.ee

CONTENTS

LIST OF ORIGINAL PUBLICATIONS

This thesis is based on the following published papers, which are referred to in the text by Roman numerals. The papers are reprinted with the kind permission of the publishers.

I Kohv, M., **Paat, R**., Lõhmus, A., & Jõeleht, A. (2023). Underground mining magnifies drought impacts in an adjacent protected raised bog. *Ecohydrology*, *16*(8). https://doi.org/10.1002/eco.2594.

II **Paat, R**., Kohv, M., & Jõeleht, A. (2022). Saturated hydraulic conductivity of boreal peat and its relationships with peat properties and sampling depth. *Hydrological Processes*, *36*(2), 1–12. https://doi.org/10.1002/hyp.14487

III **Paat, R**., Jõeleht, A., Sarap, G. S., Kohv, M. (2024). Determining peat's vertical hydraulic diffusivity and hydraulic conductivity from naturally occurring hydraulic pressure fluctuations measured at various depths. *Hydrological Processes, 38(7),* 1–14. https://doi.org/10.1002/hyp.15236

A table showing the author's contribution to the scientific papers (**'** *minor contribution*; ***** *moderate contribution*; ****** *large contribution*; ******* *leading role*).

	I	II	III
Original idea	'	**	**
Study design	'	***	**
Data collection	*	***	***
Laboratory analyses		***	***
Analysis and interpretation	**	***	***
Manuscript writing	**	***	***

1. INTRODUCTION

Peatlands are very complex and important ecosystems. They fulfill many functions in our landscapes, being a habitat for many plant and animal species (Rydin & Jeglum, 2006) and one of the most important soil carbon sinks in the world (e.g., Gorham, 1991; Nichols & Peteet, 2019; Yu et al., 2010), but also act as regulators of water flow in catchment areas (Joosten & Clarke, 2002). These are a few of many factors that necessitate the protection of these ecosystems and thus have been implemented in many nature conservation directives (e.g., Ramsar and Natura 2000). The need for conservation comes from the fact that the area of mires, as still actively peat-forming peatlands, has declined at a rate (ca 5000 km^2 annually) that is 10 times faster than the extension during the whole Holocene (Joosten & Clarke, 2002). This decline is reducing the volume of accumulated peat and with it progressively emitting CO_2 to the atmosphere (Joosten, 2009b). The main contributing factor to these problems is drainage, mainly for agriculture, forestry and peat mining (Joosten, 2009a; Paavilainen & Päivänen, 1995). Approximately 11–15% of the global peatland area has been drained (FAO, 2020), with the most notable changes occurring in Europe, where the hydrology of nearly 50% of peatlands has been altered, leading to degradation (UNEP, 2022).

Peatlands are also prevalent in the Estonian landscape. According to the latest inventory of Estonian mires (Paal & Leibak, 2011), peatlands cover approximately 22.3% of the country's territory. However, most of these peatlands are not actively peat-forming but rather degrading and thus carbon emitters, as only 5.2% of Estonian land is still covered with mires. Moreover, the extent of mires has been reduced almost 2.8 times compared to the mid-20th century, indicating a drastic change in Estonian land cover. The main contributing factors remain the same, as many mires have been drained for farmlands, manageable forests, and peat mining.

Another significant factor contributing to the global decline in peatland area is the extraction of various mineral resources in proximity or directly beneath peat formations. Notably, in Estonia, the oil-shale industry stands out as a major contributor to this phenomenon. By the end of the previous century, the oil-shale industry, in conjunction with quarry mining, had absorbed approximately 2000 hectares of peatlands (Paal et al., 1998). Beyond the readily observable effects of drainage ditches and quarries, it is essential to consider the potential indirect consequences of underground drainage on the hydraulic integrity and ecology of peatlands. The nearby mining activities can be perceived as a hidden factor capable of decreasing regional aquifer water levels, thereby posing a potential threat to the ecohydrology of peatlands (e.g., Balliston & Price, 2023; Regan et al., 2019). This concern has been a subject of discussion, particularly in northeastern Estonia, where underground oil-shale mining activities hold the capacity to impact nearby peatlands, some of which are under protection status (Marandi et al., 2013; Marandi, Veinla, & Karro, 2014; Orru et al., 2013). These concerns regarding underground drainage necessitate a comprehensive understanding of

water movement within the peat dome. Achieving this requires a thorough examination of the physical properties and hydraulic conductivity of distinct peat layers within the cross-sectional profile of peatlands.

However, estimating hydraulic conductivity could present a significant challenge, often limiting the feasibility of conducting research over a sufficiently expansive spatial domain. Commonly employed techniques for measuring hydraulic conductivity encompass both *in-situ* methodologies, such as the standpipe piezometer slug test (e.g., Baird et al., 2004; Clymo, 2004), and laboratory-based approaches utilizing permeameters (e.g., Chason & Siegel, 1986) or modified cube method (Beckwith et al., 2003). *In-situ* standpipe piezometer tests necessitate specialized equipment, including pipes equipped with intake, measuring tapes, slugs etc., while demanding rigorous adherence to testing protocols, including proper well development procedures, to minimize errors (Baird et al., 2004; Surridge et al., 2005). Moreover, the longevity of these tests presents an additional challenge, as materials with lower permeability demand extended durations for their completion (Fetter, 2001). Laboratory testing, on the other hand, is restrained by the difficulty of obtaining pristine peat samples for representative measurements. This endeavor requires the use of appropriate equipment (e.g., as detailed in Beckwith et al., 2003) and can pose formidable challenges, particularly when attempting to access deeper peat layers.

The labor-intensive, time-consuming, and challenging nature of conventional measurement methods has prompted the development of predictive models aimed at estimating peat hydraulic conductivity based on commonly measured peat characteristics (e.g., Branham & Strack, 2014; Liu & Lennartz, 2019; Morris et al., 2015, 2019; Päivänen, 1973). However, a notable observation in these studies, highlighted in the meta-analysis conducted by Morris et al., 2022, is that the majority of hydraulic conductivity measurements are typically limited to the uppermost 1 meter of peat layers, with only a few extending beyond depths of 3 meters. In the context of studying the implications of underground drainage, it becomes imperative to determine the hydraulic conductivity of the entire peat column, particularly the deepest and most compact, older, and highly decomposed peat layers. These lowermost layers are expected to exhibit the lowest conductance, playing a critical role in constraining vertical water flow under elevated vertical gradients. These considerations underscore the inadequacy of existing models, as they may not be suitable for use within these conditions. Consequently, there is a crucial need for the development of models that encompass a broader depth range to effectively address these challenges.

Additionally, it is worth noting that while there is an abundance of *in-situ* measurements of saturated hydraulic conductivity available from past studies, these measurements are often not suitable for characterizing directional flow, as they tend to primarily represent horizontal water flow (Surridge et al., 2005). Conversely, our understanding of vertical hydraulic conductivity is comparatively limited, especially of the deeper peat layers. Nevertheless, given the conditions of declining hydraulic heads in underlying aquifers and the emergence of increased vertical gradients, obtaining estimates of vertical hydraulic conductivity

becomes crucial for an accurate assessment of downward water flow. A common method for measuring directional conductance is the in-laboratory used modified cube method (e.g., Beckwith et al., 2003; Branham & Strack, 2014; Surridge et al., 2005). This method, however, necessitates the use of undisturbed peat samples, which could be difficult to retrieve, especially from deeper peats. The relatively small sampling size could also produce results that are sensitive to scale (Bromley et al., 2004; Glaser et al., 2021). To bypass the mentioned constraints, there is a compelling need for a methodology that could provide estimates of *in-situ* measured vertical hydraulic conductivity.

With this thesis, the results of a long-term monitoring of hydraulic heads in a raised bog are presented and the existence of underground drainage effects on a northeastern Estonian peatland is confirmed. The main objective is to provide valuable data about hydro-physical properties of peat and offer new and more comprehensive methods that could be useful in collecting further information about hydraulic characteristics of peat needed for assessing the resilience of peatlands to threats of underground drainage in future studies.

2. BACKGROUND OF THE STUDY AREA

The area where all the peatlands under investigation lie is situated in northeastern Estonia (Figure 1), in the lowlands of Alutaguse, where the terrain is relatively flat. The terrain, in conjunction with the humid climate, has favored the formation of peatlands in the area (Arold, 2005). Most of the peatlands are under protection while some of them form the Alutaguse National Park. These peatlands were chosen as they are located in the near vicinity of depleted, active, or potential (Koppel et al., 2018) future oil-shale mining claims (Figure 3).

The Ordovician-aged oil-shale is the most important mineral resource in Estonia, which is mainly used for generating electricity and producing oil-shale oil. Oil-shale is mined from the Estonia kukersite oil-shale deposit with an area of ca 3000 km^2 (Bauert & Kattai, 1997). The first mine was opened in 1916 (Bauert & Kattai, 1997), and production peaked in 1980 with a rate of 31.3 million tonnes annually (Raukas & Punning, 2009). Nowadays the mining rates are lower, being ca 10 million tonnes annually (Roosalu, 2023). The mining activities are creating various environmental problems in the area, the most acute being chemical pollution and dewatering of regional aquifers (Raukas & Punning, 2009), and also the deposition of huge amounts of solid alkaline waste (Bauert & Kattai, 1997) which can be seen in the local landscape.

The bedrock aquifers primarily affected by groundwater abstraction due to mining activity belong to the Ordovician aquifer system and consist of carbonate rocks of sedimentary origin. A representation of the hydrostratigraphical cross-section of the study area can be found in Figure 1. The sedimentary rocks forming the aquifers have a slight southward dip (6 to 18') (Puura & Vaher, 1997) and thus, the mined oil-shale layer is outcropping directly under the Quaternary sedimentary cover in the northern part of the study site, whereas it is situated close to 100 m deep under the southernmost peatlands.

The Ordovician aquifer system is divided into three local aquifers: uppermost Nabala-Rakvere (Nb-Rk), Keila-Kukruse (Kl-Kk), and lowermost Lasnamäe-Kunda (Ls-Kn), consisting of fractured and locally karstified limestones and dolomites. These aquifers are separated by Oandu-Keila (On-Kl) and Uhaku (Uh) aquitards which consist of clayey limestones and marls. The lateral and vertical conductivities of these carbonate aquifers are dependent on the abundance and direction of fissures and fractures in the bedrock that are decreasing with depth. In the northeasternmost corner of the study site, the Ordovician aquifers are also covered with regional Devonian-aged Narva aquitard, consisting of clayey limestones and marls (Perens & Vallner, 1997).

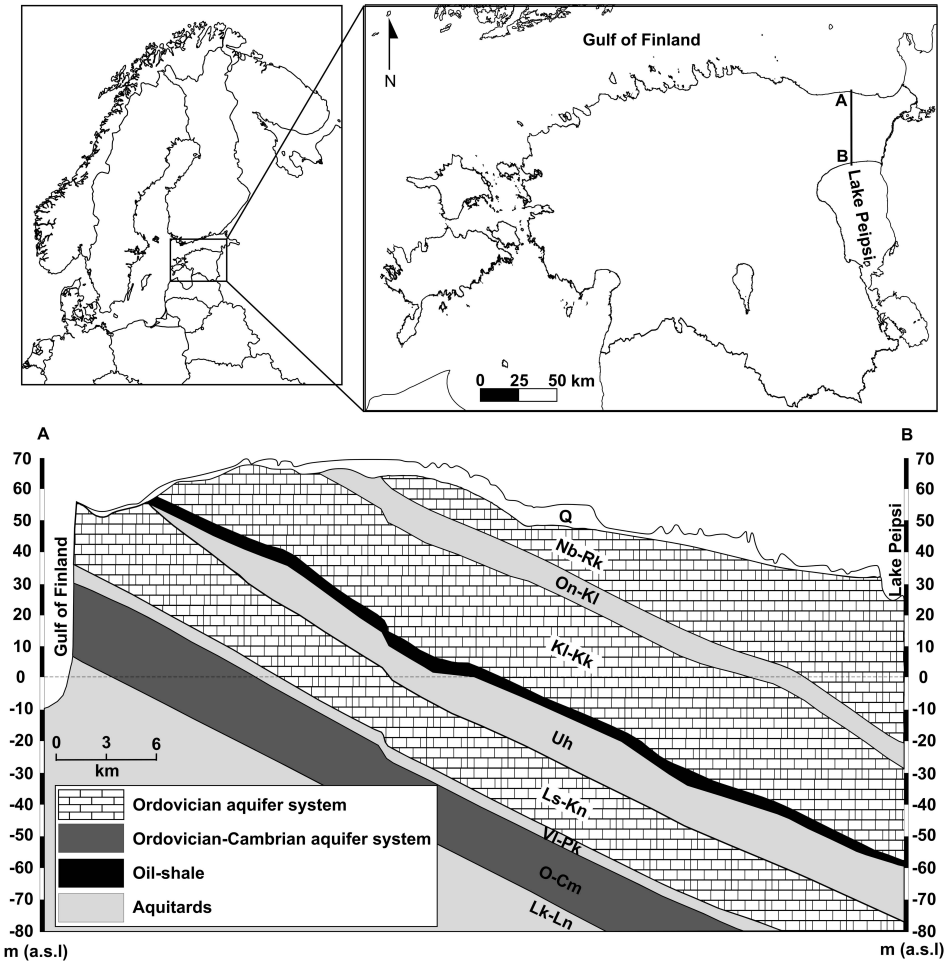

Figure 1. A hydrogeological cross-section of the study area, modified after Kattai et al., 2000, showing the major aquifer systems: Quaternary (*Q*), Ordovician (*O*) and Ordovician-Cambrian (*O-Cm*). The cross-section is cutting straight through the area, starting from the Gulf of Finland and ending at Lake Peipsi.

The bedrock is covered with Quaternary sediments containing peat, glaciolacustrine sands and silt, glaciofluvial sands, gravel, and glacial till. The thickness of the overburden is mostly less than 10 m, being thicker on glacial and postglacial landforms (Raukas & Kajak, 1997). The groundwater embedded in these sediments is strongly connected to the hydraulic head dynamics in the uppermost bedrock aquifer. These structural peculiarities are raising concerns about the possible effects of declining groundwater heads in the underlying aquifers to the hydrology of peatlands lying on top of these mineral Quaternary sediments.

Most of the peatlands can be classified as ombrotrophic raised bogs, as they elevate higher from the surrounding area and exhibit plant species common to lower-nutrient and rainwater-fed conditions (Figure 2). The peatlands surveyed in this study structurally belong to the “eastern” type bogs category. These bogs have a convex surface with a well-developed concentric pattern without steep slopes (Masing, 1984). The researched peatlands also include bog complexes (such as Puhatu, Selisoo, and Sirtsi bog complexes) that consist of different bog domes and are intertwined with areas of different trophic conditions, such as transitional mires. The sites are surrounded by forestry drainage while having their central bog area still intact.

Figure 2. The landscape in Selisoo raised bog, exhibiting a bog pool. Photo by Marko Kohv.

3. MATERIAL AND METHODS

3.1 Data and sample acquisition from peatlands

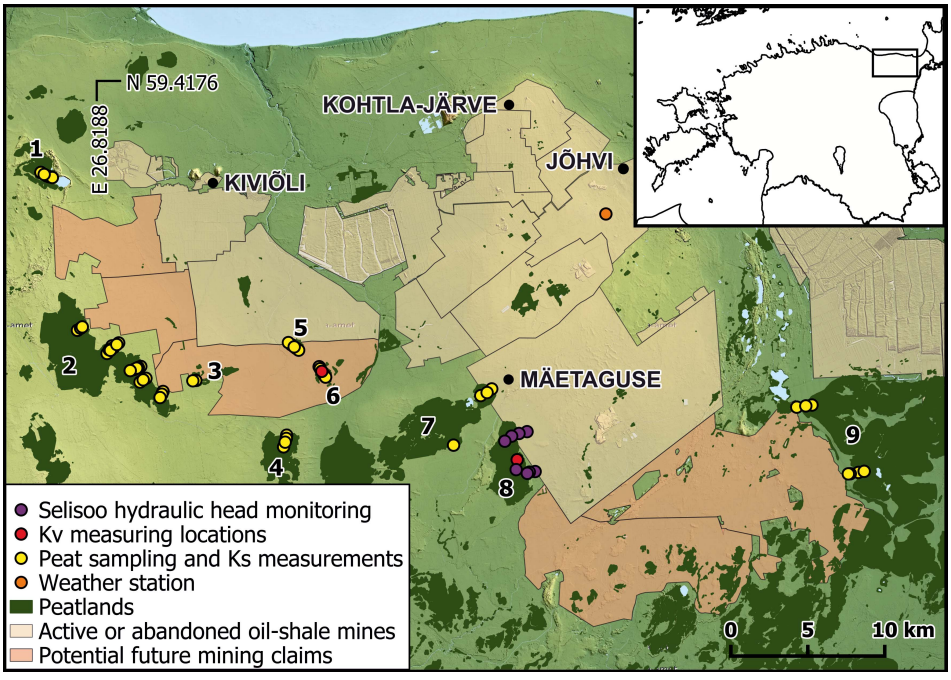

Figure 3. Sampling locations of different data used in paper I–III, nearby oil-shale mining claims (active, abandoned or potential) and Jõhvi weather station (N 59.3289, E 27.3983). Bogs: 1 – Uljaste, 2 – Sirtsi, 3 – Tedresoo, 4 – Virunurme, 5 – Oandu, 6 – Kaasiksoo, 7 – Ratva, 8 – Selisoo and 9 – Puhatu. Base maps from Estonian Land Board.

The water level monitoring data used in Paper I originates from Selisoo bog (no 8 in Figure 3), which lies in the proximity of an active underground oil-shale mine named “Estonia”. The hydraulic head monitoring network in the bog and underlying main bedrock aquifers was established in 2010. The locations of the monitoring points in Selisoo are shown in Figure 3. A more detailed schematic of the monitoring network can be found in PAPER I – Kohv et al. (2023). The network includes every aquifer between the surface of the mire and the bottom of the oil-shale underground mine. The network consists of two transects extending from the eastern boundary of the Natura 2000 conservation site to the centers of the two discernable northern and southern bog domes. The transects include every zone of the peatland: (i) the drained peatland forest (former transitional mires and swamps), (ii) a transitional area between the drained peatland forest and undrained bog, (iii) the forested bog slope on the bog dome, and (iv) the semi-opened center of the bog dome. The pressure heads in the Ordovician aquifers were measured with observation wells located at the edge of the Selisoo research area, using

sensors logging automatically with an 8-hour interval. The hydraulic heads in the Quaternary cover were measured using "push-in" electronic piezometers with a 3 cm screened interval, also logging with an 8-hour interval. The piezometers were installed in most of the measuring locations in pairs, one measuring hydraulic head in peat (at 2 m depth) and the other in the underlying mineral sediments directly beneath the peat. Simultaneous atmospheric pressure was measured on site. The data used in the analysis was collected from 2010 until the end of 2021.

3.1.1 Peat sampling and saturated hydraulic conductivity measurements

The peat sampling and hydraulic conductivity measurements for PAPER II were carried out in several raised bogs in the study region (Figure 3). The sampling locations were arranged on transects that extend from the last drainage ditch at the margin of the bog to the intact center, having 150–250 m distance between points depending on the locations of present general subtypes. The coring of peat was done with a half-cylindrical Russian-type corer with a 5.3 cm diameter and a meter long sampling window. Peat samples were gathered from every discernable and at least 5 cm thick peat layer for laboratory analyses.

The saturated hydraulic conductivity tests in peat were carried out in the near vicinity of the locations where the peat coring and sample collection were done. Two types of hydraulic conductivity tests were performed using BAT-permeameters (Torstensson, 1984) and falling head piezometer tests (Figure 4). The permeameters were used to measure conductivity in less conductive, more decomposed, and consequently deeper peat layers, whereas piezometer tests were carried out in the upper, more conductive, less decomposed peat. The falling head tests were carried out by pouring a known volume of water into PVC piezometers with a 10 cm long perforated intake while measuring the water level recovery with an automatic pressure transducer. The hydraulic conductivity from piezometer tests was calculated according to Hvorslev (1951).

Figure 4. Measuring saturated hydraulic conductivity with BAT-permeameters and piezometer (beige PVC pipes in the picture) tests.

3.1.2 Hydraulic heads and peat samples for estimating vertical hydraulic properties of peat

The data for vertical hydraulic properties estimation was gathered from two raised bogs in the study area: Kaasiksoo bog (no. 6 in Figure 3) and Selisoo bog (no. 8 in Figure 3). These sites display different peat column thicknesses being 3.4 m in Kaasiksoo and 5.3 m in Selisoo. Prior to any equipment installment, peat cores were retrieved from both locations for subsequent laboratory analyses of peat properties and compressibility. The peat was cored to the underlying mineral sediments using a Russian-type corer with a 5.3 cm diameter. The samples were kept in halved PVC pipes wrapped in cling film (for bulk density and humification analyses) and in sample bags (compressibility samples).

The hydraulic pressures with buried pressure transducers were collected from the same locations. In Kaasiksoo, the heads were measured at 3.0 m, 3.2 m, and 3.4 m, and in Selisoo at 4.8 m and 5.3 m. For hydraulic pressure measurements, automatic sensors with a 20 mH_2O pressure range were used. As these sensors are not designated for burial into sediments, special 3D-printed casings were constructed in which the sensors were placed during installation and hydraulic pressure measurements. Simultaneous air pressure measurements were collected from both sites.

3.2 Laboratory measurements

All the gathered peat samples for PAPER II and PAPER III were kept refrigerated until commencing the analyses. Dry bulk density (*BD*), organic matter content (*OM*), and humification (*HUM*, for the characterization of degree of decomposition) were measured for every taken sample following the *ACCROTELM* protocol by Chambers et al. (2011). First, the wet samples were oven-dried at 105 °C for the *BD*. Then, the dried samples were ground and divided approximately in half, of which the first half was burned in a muffle furnace at 550 °C for *OM*, and the second one dissolved in 8% NaOH solution for the extraction of the humic acids. The light absorbance (*HUM*) of the extracted humic acids was measured with a HALO RB-10 spectrophotometer.

The compressibility of peat for PAPER III was assessed with a standard oedometer test (*ISO 17892-5:2017*). The oedometer tests were carried out using the *Matest S260* front-loaded oedometer. The samples in the ring were imposed to weights ranging from 250 g to 4000 g, which constitutes applied forces of 5.55 kPa to 88.73 kPa. The adding and removing of weights was done gradually, each settlement or recovery lasting for 24 h. The vertical strain was measured with the provided automatic digital dial gauge and checked manually using a digital caliper. Before the first and after each sequent settlement, the vertical saturated hydraulic conductivity of the peat sample was measured (*ISO 17892-11:2019*). The coefficients of compressibility for each sample were calculated from the slope of the rebound curve of the consolidation test results showing the change in vertical strain with the applied or removed effective stresses.

3.3 Statistical analyses

All the statistical analyses were made using the *R* programming language (R Core Team, 2023) in *R-studio* integrated development environment. A $p\text{-}value < 0.05$ was used for all the statistical tests used in different applications.

3.3.1 Time-series analysis in Selisoo

The collected hydraulic head time-series from Selisoo monitoring system were first imputed, as some contained data gaps formed during the long survey period. The imputation was carried out using EMB (expectation-maximisation with bootstrapping) algorithm, which has been implemented in *Amelia* II (Honaker et al., 2011) package. The imputed time-series were then decomposed to distinguish different trend components for finding the effects of underground drainage associated with nearby mining activity. For decomposition, the STL algorithm (Cleveland et al., 1990) from the *R stats* package was used. The time series were also subjected to trend testing to further confirm drawdowns in the measured hydraulic heads. Trend testing was carried out with *Theil-Sen* nonparametric model, recommended by the US Geological Survey (Helsel et al., 2020) found in

the *Openair* package (Carslaw & Ropkins, 2012). To define the breakpoints of significant variance and/or mean change in the measured time series, *breakpoints* function in *strucchange* (Zeileis et al., 2002) package was used. To assess the weather effects during the survey period, the temperature and precipitation data over the survey period (2010–2021) and historical measurements (1980–2010) from a nearby Jõhvi weather station were acquired. To assess the severity of drought during this period the precipitation-evapotranspiration index (SPEI) was calculated using *SPEI* package (Vicente-Serrano et al., 2010) in combination with Thornthwaite equation (Thornthwaite, 1948).

3.3.2 Predictive models for saturated hydraulic conductivity.

The predictive statistical models for indirect assessments of saturated hydraulic conductivity proposed in PAPER II – Paat et al., 2022 were constructed as follows. Linear mixed effects (LME) models were opted for the prediction of saturated hydraulic conductivity (K_s) from peat physical characteristics (BD, von Post score, HUM, depth, and botanical composition). The fitting was done using the *nlme* package (Pintero et al., 2020) and following a "top-down" selection strategy described in Zuur et al. (2009). A randomly selected sample (counting for 20% of the whole dataset) was removed from the initial data to serve as an independent test set for later model validation.

The *von Post* score was treated as a continuous variable during the fitting process to give the models more degrees of freedom, which consequently provides greater explanatory power and quality, as was also suggested by Morris et al. (2019). The botanical composition of peat was treated as a categorical value (*phase*) and characterized by three categories dependent on their growth period trophic conditions (minerotrophic, transitional, and ombrotrophic). Due to the non-linearity of K_s and measurement depth with other variables, the parameters were transformed to a logarithmic scale ($\log_{10}$).

Two *LME* models were fitted using the training data: one using the *von Post score and the* other *HUM* for describing peat decomposition. The "top-down" selection process started with an all-inclusive fixed effects model that contained the independent variables (*BD*, *von Post* score or HUM, $\log_{10}$(*depth*) and *phase*), and interaction terms between. Next, the random component structure was chosen by adding random effects in a stepwise manner and comparing each new model performance with *Restricted maximum likelihood estimation*. After finding the optimal random structure, the fixed effects structure of the model was sorted out, by gradually removing interaction terms and variables from the model and comparing each new model with the previous one, using *Likelihood ratio testing*. The performance of the final *LME* models was assessed with the conditional (variance explained by the whole *LME* model) and marginal (variance explained by the fixed effects only) variance (r^2) (Nakagawa & Schielzeth, 2013) using *squared-GLMM* function in the *MuMIn* package (Barton, 2020). The fit between measured and predicted $\log_{10}(K_s)$ values was evaluated with root mean square error (*RMSE*).

3.4 Vertical hydraulic properties estimation

The estimation of vertical hydraulic properties from the measured hydraulic heads in Selisoo and Kaasiksoo in PAPER III started with the calculation of vertical hydraulic diffusivity. The diffusivity was calculated using a 1D – analytical solution (see eq. 7 in Dong et al. (2012) or eq. 2 in PAPER III – Paat et al., 2024). A numerical code in Python was written for the implementation of the mentioned solution. This analytical solution allows for the calculation of hydraulic head response in time at a depth from a reference source, where the *in-situ* time-series data is measured. The vertical hydraulic diffusivity (D) value was produced by fitting the calculated hydraulic heads time-series with the *in-situ* measured hydraulic heads at the designated depth. The best fit was evaluated with *RMSE* between the calculated and measured time-series. A more detailed description of the calculation methodology can be found in PAPER III. The vertical hydraulic conductivity was determined using the calculated diffusivity values and the specific storage of peat, which was determined through laboratory-measured coefficients of compressibility.

4. IMPACTS OF UNDERGROUND DRAINAGE ON A RAISED BOG

4.1 Hydraulic heads in the bedrock aquifers

The data from monitoring wells in Selisoo raised bog (Figure 5) clearly indicate a decline in hydraulic heads in both bedrock aquifers that are situated between the oil-shale layer and Quaternary sediments on top. The most prominent drainage influences are seen in the Kl-Kk aquifer (wells M2 and L2), which contains the oil-shale layer and where the actual mining is taking place. A more subtle but still visible drop in hydraulic heads also occurs in the Nb-Rk aquifer (wells M1 and L1), which is separated from the latter with On-Kl aquitard and is directly below the Quaternary aquifer. The dynamics of the declines are different amidst the two monitoring transects that is related to the development of the oil-shale mine. The decrease in hydraulic heads started already before the establishment of the monitoring system in the southern part of the peatland (L1 and L2), however between 2012 and 2015 a further 12 m decline followed in Kl-Kk aquifer, eventually stabilizing with an increase in seasonal fluctuations. In the upper Nb-Rk aquifer, the declines were very subtle, approximately 1 m since 2012. A more distinct drainage response is observed in wells situated at the northern transect (M1 and M2). The first prominent 2 m decline in Kl-Kk aquifer happened between 2010 and 2012, while mining took place approximately 0.5 km to the east of the monitoring wells. A more abrupt change was observed in 2014, with more than a 10 m drop in total heads, which could be related to the excavation of the first transport and drainage tunnels within 100 m of the monitoring wells. The drop in the upper Nb-Rk aquifer was smaller, showing a decline of approximately 2 m since 2014. A more noticeable change in the upper limestone aquifer has been the appearance of high seasonal variability in the hydraulic heads (PAPER I – Kohv et al., 2023).

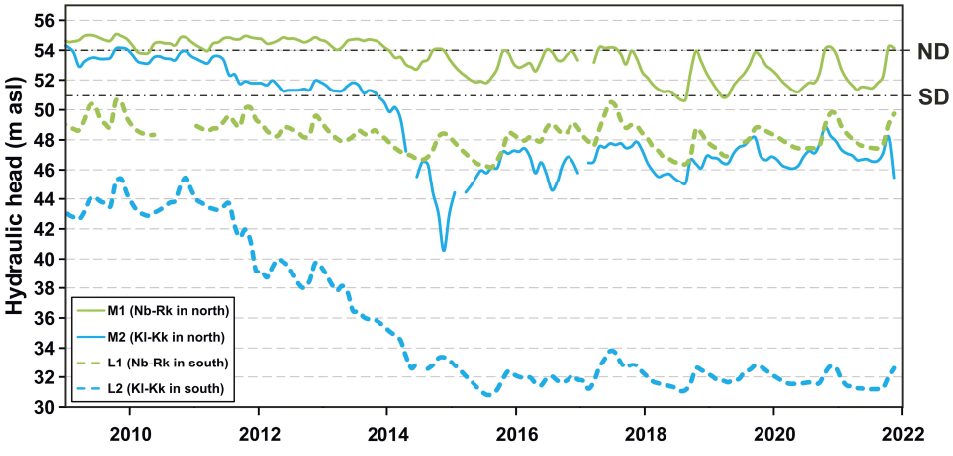

Figure 5. Monthly average groundwater levels in the bedrock aquifers lying between the oil-shale layer and Quaternary sediments. *ND* denotes the altitude of the bottom of the ditches next to the monitoring wells at the beginning of the northern transect and *SD* at the southern transect (PAPER I – Kohv et al., 2023).

4.2 Hydraulic head changes in Selisoo bog

Figure 6 expresses the monthly averaged hydraulic heads measured in the Quaternary aquifer on both the monitoring transects with calculated trendlines and corresponding Theil-Sen trend tests *p-values* and results of the breakpoint analysis. A more comprehensive results of the Theil-Sen analysis can be found in the Supplementary Materials in PAPER I – Kohv et al., 2023.

Most of the monitoring points encountered a decline in hydraulic heads during the given survey period. In peat at the two distinct bog domes, the water levels showed stable (N4T, *p-value* > 0.05) or even slightly increasing (S4T, *p-value* < 0.05) trends over the study period, while in the underlying Quaternary aged mineral sediments (N4M and S4M) the hydraulic heads were declining significantly (negative trend with *p-value* < 0.05 for both). It is worth mentioning that S4M experienced one of the largest observed declines among the monitoring points in the Quaternary aquifer. On the bog slopes, a significant decline in hydraulic heads was observed in the northern transect (N3T, p-value < 0.05), while no significant trends were present on the southern transect (S3T, *p-value* > 0.05). In the underlying sediments, there was a significant negative trend (*p-value* < 0.05) seen in the hydraulic heads on the northern transect (N3M), while it showed a more dynamic, but similar as in peat non-significant (*p-value* > 0.05) trend implications in the south (S3M). The data originating from the monitoring points in the drained forest surrounding the bog mostly exhibited declines in the hydraulic heads. There is a clear and significant drop seen in both Quaternary aquifers at the northern transect (N1T, N2T, and N2M), however at the southern one, the declines are not as pronounced, being significantly present in S2T, while being relatively stable in S1T (PAPER I – Kohv et al., 2023).

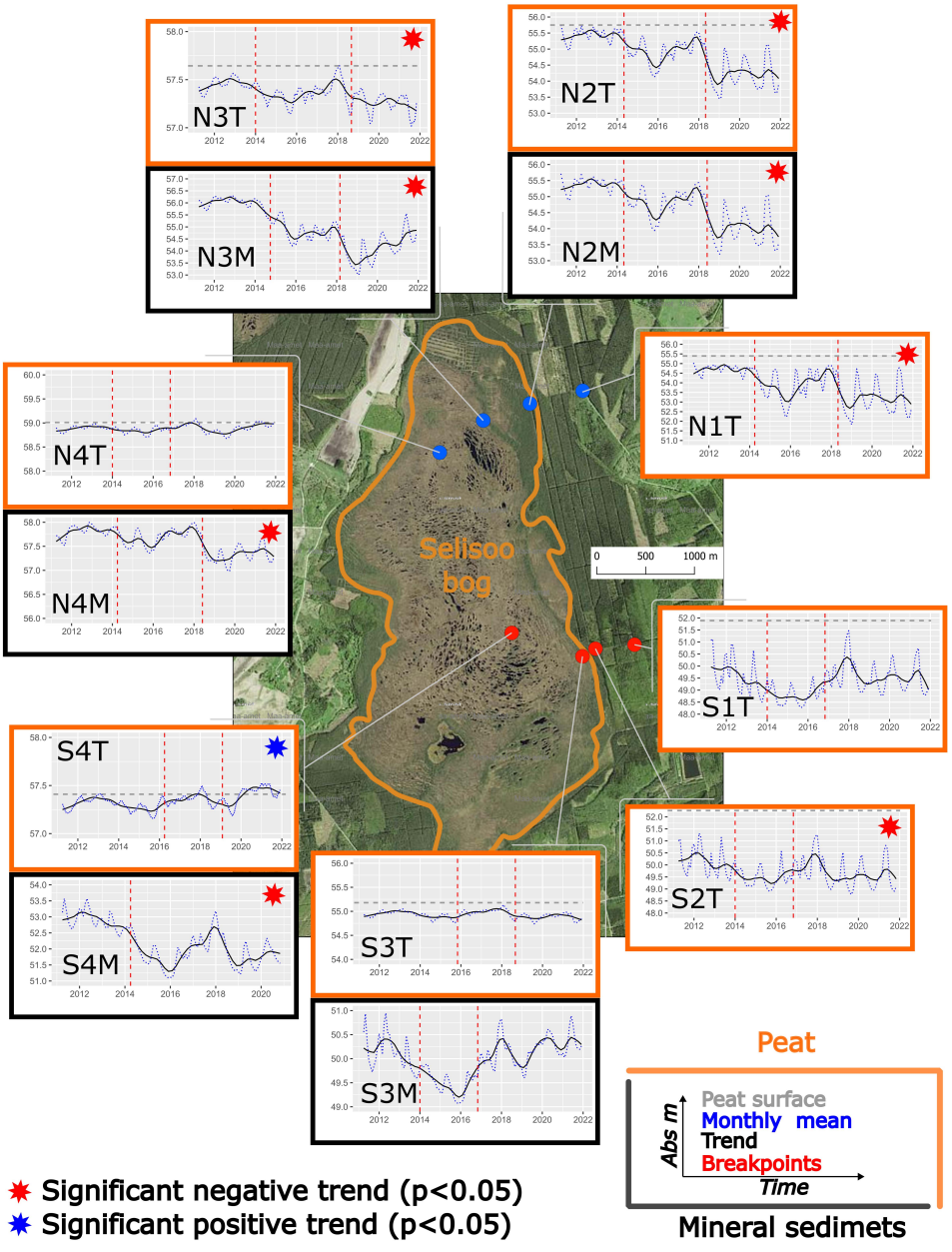

Figure 6. Results of the hydraulic head monitoring in the Quaternary aquifer, in peat (T) and mineral (M) sediments at the northern (N) and southern (S) transect. In the background is orthophoto of the Selisoo raised bog acquired from the Estonian Land Board (Paper I – Kohv et al., 2023).

4.3 The effects of underground drainage on Selisoo

From the monitoring results it is evident that the increased drainage within the Kl-Kk aquifer is transferred towards the upper limestone formations and Quaternary aquifer. The Oa-Kl aquitard proves inadequate in fully separating and isolating these two bedrock aquifers subsequently resulting in diminished hydraulic heads in the Nb-Rk aquifer. The drainage effects are also transmitted through the glacial Quaternary sediments, as concurrent head declines are detectable directly under the peat. This shows that the water bound into the Quaternary aquifer is directly dependent on the changes within the underlying bedrock (PAPER I – Kohv et al., 2023).

However, when comparing the hydraulic head movements measured in peat and directly beneath it in the Quaternary aquifer, an apparent pattern emerges. When examining the hydraulic heads measured at the bog center (N4 and S4), it becomes evident that the overall fluctuation dynamics and amplitude differ between the measurements in peat and in mineral sediments, indicating more stable conditions in the peatland. This distinct separation is also noticeable at the forested bog slope (N3 and S3) but diminishes moving towards the bog margins, as the hydraulic heads show very similar dynamics (N2T and N2M) (PAPER I – Kohv et al., 2023).

The similarities in the hydraulic head fluctuation dynamics between N2T and N2M indicate that these two piezometers, although placed at different depths, characterize hydraulic heads in the same aquifer (Figure 6). This suggests that the peat layer between them is insufficient to separate these two sediment layers, while it seems to be sufficient when moving towards the centers of the bog domes, where the thickness of peat increases (PAPER I – Kohv et al., 2023). Given the definitive connection between transmittance and overall thickness of the peat dome, the isolative properties of peat diminish near the bog margins (PAPER I – Kohv et al., 2023), like in Selisoo where peat layers thin out (Hiiemaa et al., 2014). Additionally, it's important to recognize the spatial heterogeneity of peat thickness. Cross-cutting structures, such as cracks, sinkholes (Kværner & Snilsberg, 2011), calcareous bioherms (Balliston & Price, 2023), and buried eskers (Comas et al., 2011), could disrupt the integrity of the peat and create pathways through which water can flow more rapidly from the peat surface to the underlying sediments and bedrock (PAPER I – Kohv et al., 2023).

The long-term hydraulic head monitoring and observed declines at the bog slopes and in the drained peatland forest surrounding Selisoo, particularly those noted on the northern transect, suggest that mining-induced bedrock aquifer drainage has effects on this peatland (PAPER I – Kohv et al., 2023). This raises concerns regarding the integrity and preservation of other peatlands in the region in response to any potential underground disturbances, whether anthropogenic or climatic. Prior knowledge about the structure and hydrology of peatlands is crucial from an environmental conservation standpoint. Such knowledge facilitates the construction of comprehensive hydrological/hydrogeological models, which are essential for understanding and predicting water movement within the

peatland and between underlying units during aquifer depressurization. The thickness of the peat is one critical element determining the connectivity of the peat surface with the underlying sediments and the severity of underground drainage influences. It is intricately linked with its physical properties, which shape the saturated hydraulic conductivity. Therefore, it is of utmost importance to learn and gather information about the hydro-physical properties of peat, which are necessary for determining and understanding water movement in such hydro-geologic conditions (PAPER I – Kohv et al., 2023).

5. PEAT PROPERTIES AND SATURATED HYDRAULIC CONDUCTIVITY

5.1 Physical properties of peat in the study sites

The variations in peat physical properties with depth are illustrated in Figure 7. More precise descriptive statistics for the peat parameters can be found in Table 1 of PAPER II – Paat et al. (2022). The depth across all collected samples (in total 201) ranged from 0.15 m to 6.50 m. The measured dry bulk density (*BD*) values ranged between 0.02 and 0.25 g cm^{-3}, with the highest estimated value observed in the minerotrophic fen peat.

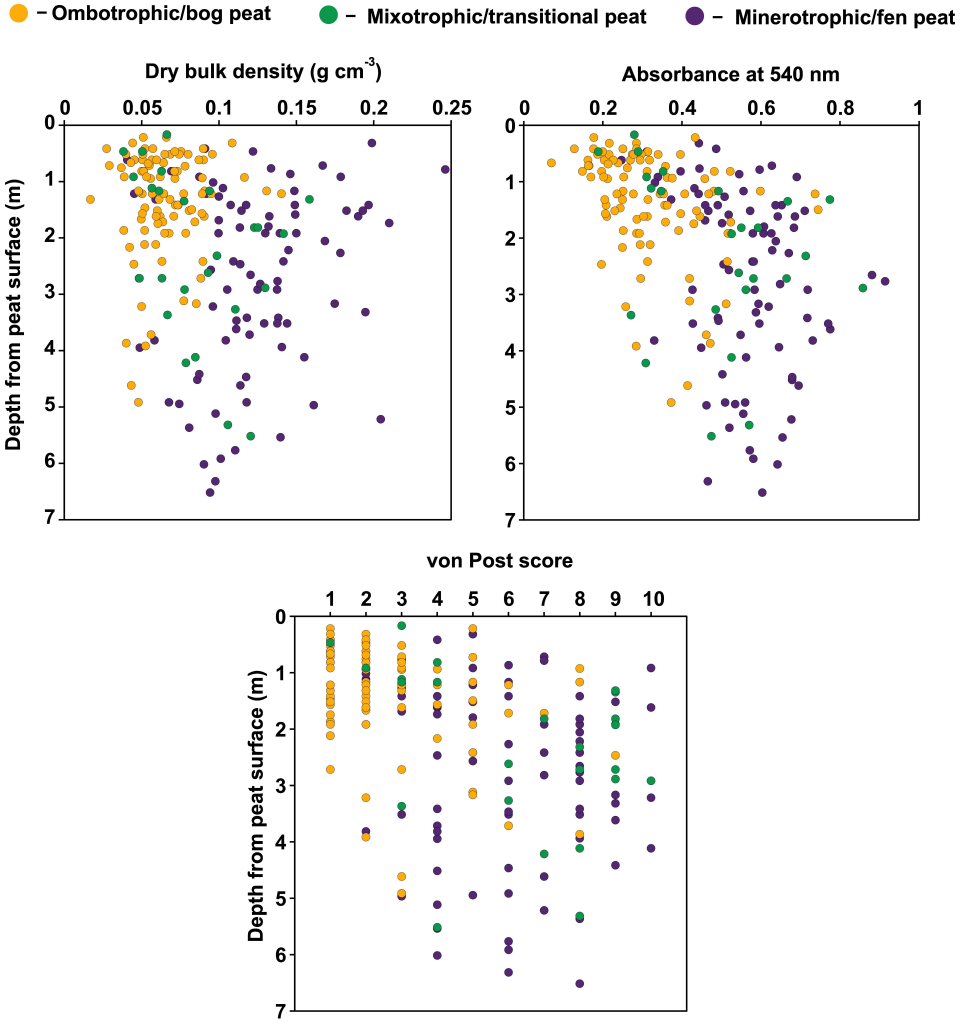

Figure 7. Dry bulk density and degree of decomposition, on von Post scale and as absorbance of alkali extracted humic acids or humification (*HUM*) as a function of sampling depth in different peat types. The figures are constructed with data from PAPER II – Paat et al. (2022).

Additionally, the minerotrophic fen peat exhibited the highest average *BD* values across all study sites. This observation aligns with the overall structure of raised bogs in the area, as plant remnants (mostly sedges, reeds, and wood remains) deposited during minerotrophic conditions can be found in the bottommost layers of the peatlands, thus becoming more humified and compacted. Conversely, the more surficial peat layers, dominated by ombrotrophic bog peat, showed the lowest *BD* with a mean of 0.06 g cm^{-3}, consisting mostly of decayed *sphagnum* mosses and hare's-tail cotton grass *E. Vaginatum*. The decomposition state of the samples varied widely, exhibiting *von Post scores* from H1 to H10 and humification ranging from 0.07 to 0.91. Notably, the more recently deposited ombrotrophic bog peat clearly exhibited a lower decomposition state compared to the older peat formed during mixotrophic and minerotrophic conditions.

5.2 Saturated hydraulic conductivity

The correlation of saturated hydraulic conductivity with sampling depth, *BD, von Post score*, and *HUM* are pictured in Figure 8. The correlation coefficients between them can be found in Table 1. The *in-situ* measured saturated hydraulic conductivity fluctuates in a range of 2.0×10^{-10}–6.1×10^{-4} m s^{-1}, with the highest values being in ombrotrophic peat (2.4×10^{-4} m s^{-1}) and the lowest in minerotrophic (2.0×10^{-10} m s^{-1}) (PAPER II – Paat et al., 2022). There is no clear correlation between measurement depth and $\log_{10}(K_s)$. It appears that, up to a certain depth, the saturated hydraulic conductivity exhibits a linear decrease, reaching a plateau beyond which the $\log_{10}(K_s)$ values predominantly fluctuate within the range of 1.0×10^{-8} to 1.0×10^{-10} m s^{-1} (PAPER II – Paat et al., 2022).

It is apparent that more densely compacted peat (indicated by higher *BD* values) exhibits lower saturated hydraulic conductivity, which also correlates with the degree of decomposition. The lowest measured conductivity values fall within the range of H7–H10 on the *von Post* scale, while the highest $\log_{10}(K_s)$ values were determined in less decomposed peat layers (H1–H5). Overall, there is a negative correlation between saturated hydraulic conductivity and other measured peat properties. Specifically, there is no clear linear correlation between measurement depth and $\log_{10}(K_s)$, as indicated by a relatively low correlation coefficient. The strongest correlation is observed between $\log_{10}(K_s)$ and humification (*HUM*) (Table 1), showing a decrease in conductivity with rising light absorption values. The correlation of *von Post score* closely resembles that with *HUM*. Dry bulk density demonstrates a lower but moderate correlation with $\log_{10}(K_s)$ (PAPER II Paat et al., 2022).

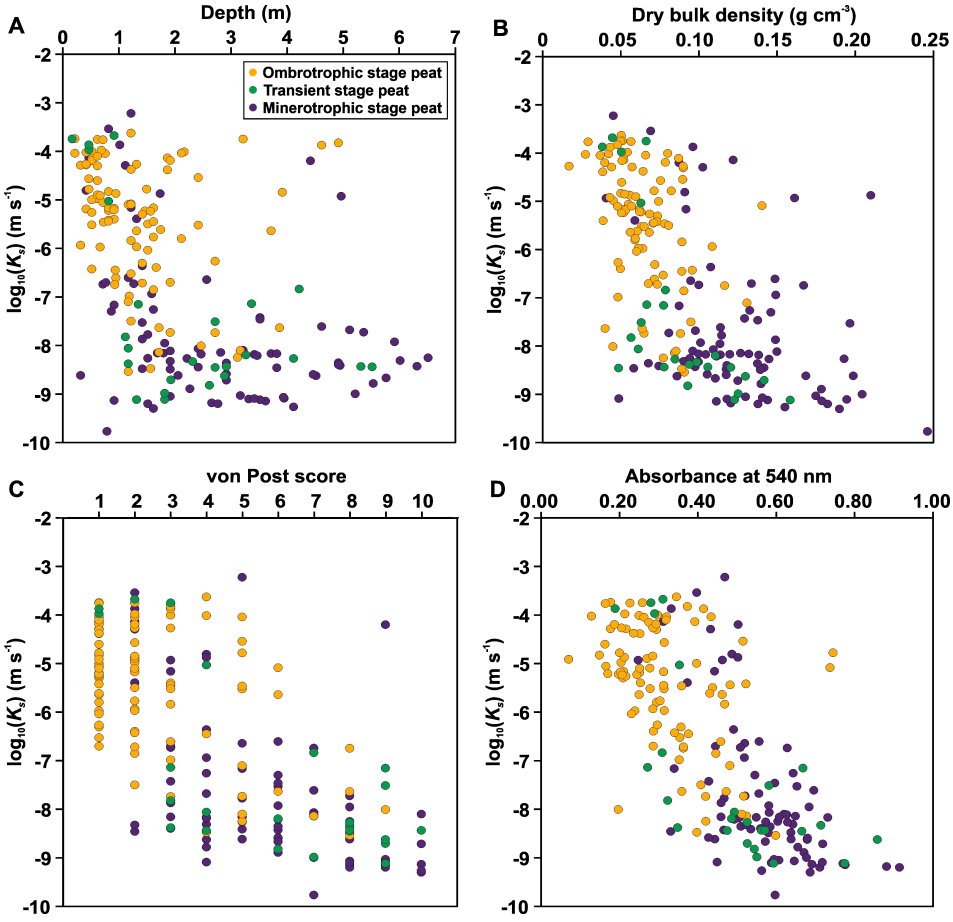

Figure 8. Correlation of $\log_{10}(K_s)$ with depth, dry bulk density, degree of decomposition and humification (absorbance at 540 nm) (PAPER II – Paat et al., 2022).

Table 1. Pearson's correlation coefficients of the physical properties (dry bulk density, BD; light absorbance at 540 nm, HUM) with $\log_{10}(K_s)$ (PAPER II – Paat et al., 2022).

	Depth	BD	von Post	HUM	$\log_{10}(K_s)$
Depth	1				
BD	0.21*	1			
von Post	0.44**	0.58**	1		
HUM	0.47**	0.69**	0.78**	1	
$\log_{10}(K_s)$	–0.51**	–0.62**	–0.72**	–0.73**	1

Note. *Correlation is significant at the 0.05 level and ** correlation is significant at the 0.01 level.

The negative correlations seen between the $\log_{10}(K_s)$ and measured physical properties coincide well with the findings of previous studies (e.g., Branham & Strack, 2014; Morris et al., 2019; Päivänen, 1973). The change in saturated hydraulic conductivity with depth is quite complex. The absence of a clear correlation is in agreement with numerous other studies, summarized by a meta-study conducted by Morris et al. (2022). The results of this study (Figure 8A) and of Morris et al. (2022) clearly show that hydraulic conductivity at the same depths over measuring sites can vary quite remarkably, over several orders of magnitude. Regardless of the depth, the fen peat exhibits generally lower hydraulic conductivity than bog peat, however, it is very important to note that deeper lying peat layers may exhibit K_s values as high as more surficial peat (PAPER II – Paat et al., 2022). The highly heterogeneous distribution of saturated hydraulic conductivity with depth is expected when samples are collected over multiple peatlands and from various locations. Each peatland develops under a unique combination of geomorphological, climatic, and hydrological/hydrogeological conditions, leading to variations in peat deposit thickness and heterogeneity in physical properties (McCarter et al., 2020; Xia et al., 2019).

The apparent decrease in $\log_{10}(K_s)$ with decomposition and dry bulk density clearly reflects the change in the pore structure of peat with an increase in overall compaction and plant litter decay (McCarter et al., 2020; Rezanezhad et al., 2010, 2009). However, it should be noted that botanical composition still plays a significant role in shaping the hydraulic structure of peatlands. In these study sites, lower conductivity values were measured in peat consisting of plant remains deposited during minerotrophic and mixotrophic conditions, whereas highly decomposed bog peat, buried during ombrotrophic conditions, exhibited higher conductivity (Figure 8). The visually very decomposed and thus texturally amorphous wood peat, mostly deposited during minerotrophic and mixotrophic (transitional) conditions, appears to be one of the most important contributors to the lowest measured $\log_{10}(K_s)$ values (PAPER II – Paat et al., 2022).

6. PREDICTIVE MODELS FOR SATURATED HYDRAULIC CONDUCTIVITY

6.1 Model using von Post score.

The first predictive model was built using the *von Post* score as one of the variables, omitting *HUM* from the selection process. To test for any within-core dependency effects the core location as identificator variable (*ID*) was also included. The stepwise model fitting process yielded a linear mixed effects (*LME*) model that utilizes all the predictor variables as fixed effects but also a random intercept and a slope. Based on likelihood ratio testing, the inclusion of core *ID* as a random intercept substantially enhanced the performance of the original model, initially comprising only fixed effects ($L = 5.222$, $df = 1$, $p = 0.022$). The selection process also revealed a noteworthy enhancement when introducing a random slope to the model, altering the influence of $\log_{10}(depth)$ on $\log_{10}(K_s)$ based on the peat core (*ID*) ($L = 9.491$, $df = 2$, $p = 0.009$). However, none of the other combinations of random slopes with the random intercept yielded a substantial improvement in the model's performance compared to the initial fixed effects model (likelihood ratio test, $p > 0.05$ in all cases) and thus were omitted (PAPER II – Paat et al., 2022).

None of the examined fixed-effects interactions demonstrated significance as predictors (*BD*×*phase*, $F_{(2, 98)} = 0.167$, $p = 0.847$; *von Post*×*phase*, $F_{(2, 98)} = 0.621$, $p = 0.540$; $\log_{10}(depth)$×*phase*, $F_{(2, 98)} = 0.033$, $p = 0.968$). Furthermore, none of these interactions significantly enhanced the predictive capability of this *LME* model based on sequential likelihood ratio tests (*BD*×*phase*, $L = 0.744$, $df = 1$, $p = 0.689$; *von Post*×*phase*, $L = 0.900$, $df = 1$, $p = 0.638$; $\log_{10}(depth)$×*phase*, $L = 0.084$, $df = 1$, $p = 0.959$). To avoid overfitting, all non-significant interaction terms were excluded from the model (PAPER II – Paat et al., 2022). The population-level model for $\log_{10}(K_s)$ is summarized in Table 2, while the coefficients of intercepts and slopes of $\log_{10}(depth)$ for various peat cores could be studied further from the supplementary materials in PAPER II – Paat et al., 2022.

The model fitting process reveals a coring site (ID) dependency that has a random effect on the models' intercept, characterized by a variance of $\sigma^2 = 0.15$. Similarly, the influence of $\log_{10}(depth)$ on $\log_{10}(K_s)$ varies among peat cores, exhibiting a variance of $\sigma^2 = 1.31$. The fixed-effects structure of the model reveals that there is a notable decrease in $\log_{10}(K_s)$ of peat with an increase in *BD*, *von Post score*, and $\log_{10}(depth)$. However, the categorical variable (*phase*), allocating plant species in the remains of peat that have lived during similar trophic conditions (groundwater or rainwater fed), did not demonstrate a significant independent effect on $\log_{10}(K_s)$. The fitted *LME* model describes a substantial portion of the variance in $\log_{10}(K_s)$ (conditional $r^2 = 0.77$), although the majority of variance is explained by the fixed effects only (marginal $r^2 = 0.66$) (PAPER II – Paat et al., 2022).

Table 2. Summarization of the first predictive model for $\log_{10}(K_s)$ (m s^{-1}) using *von Post* score as a descriptor variable for characterizing peat decomposition state.

Descriptor variable	Category	Coefficient	Standard Error	F	Significance
Intercept		–3.850	0.371	4060	<0.001
BD (g/cm^3)		–15.749	2.800	191.1	<0.001
von Post score		–0.191	0.044	70.10	<0.001
$\log_{10}$(*depth*) (m)		–2.049	0.361	32.09	<0.001
phase		–	–	2.251	0.110
	min	–	–	–	–
	trans	–0.571	0.280	–	–
	omb	–0.133	0.265	–	–

Note: Each *phase* variable category is encoded as a dummy variable with a value of 1 if it signifies the mentioned condition, and 0 otherwise. The minerotrophic category serves as the reference, rendering its level redundant. Marginal $r^2 = 0.66$, conditional $r^2 = 0.77$.

6.2 Model using Humification

The second model using *HUM* as an independent variable instead of *von Post* score gave similar results to the first one (Table 3). Using likelihood ratio testing, the effectiveness of the original fixed effects model demonstrated a notable enhancement upon the inclusion of core ID ($L = 7.936$, $df = 1$, $p < 0.005$) and $\log_{10}$-transformed sampling depth ($L = 8.230$, $df = 2$, $p = 0.016$) within the random structure of the model. No other pairings of random slopes with the random intercept yielded a statistically significant improvement in model performance compared to the initial fixed-effects model (likelihood ratio test, $p > 0.05$ in all instances) (PAPER II – Paat et al., 2022).

As with the first model, none of the fixed-effects interactions were significant predictors (*BD*×*phase*, $F_{(2,\ 98)} = 0.950$, $p = 0.390$; *HUM*×*phase*, $F_{(2,\ 98)} = 1.930$, $p = 0.151$; $\log_{10}$(*depth*)×*phase*, $F_{(2,\ 98)} = 0.321$, $p = 0.726$). Moreover, none of the fixed-effects interactions improved the model according to the likelihood ratio testing (*BD*×*phase*, $L = 0.264$, $df = 1$, $p = 0.877$; *HUM*×*phase*, $L = 5.790$, $df = 1$, $p = 0.055$; $\log_{10}$(*depth*)×*phase*, $L = 0.627$, $df = 1$, $p = 0.731$). Unlike with the previous model, the categorical variable *phase* representing the botanical composition is a significant ($p < 0.05$) explanatory variable (PAPER II – Paat et al., 2022).

Table 3. Summary of the second *LME* model for predicting $\log_{10}(K_s)$ in ms^{-1}. This model uses the absorbance of light at 540 nm in alkali-extracted humic acids as a descriptor of the degree of decomposition.

Descriptor variable	Category	Coefficient	Standard Error	F	Significance
Intercept		–3.632	0.430	3411	<0.001
BD (g/cm^3)		–15.642	3.073	180.9	<0.001
HUM		–2.548	0.772	57.685	<0.001
$\log_{10}$(*depth*) (m)		–2.010	0.387	29.40	<0.001
phase		–	–	4.436	0.014
	min	–	–	–	–
	trans	–0.683	0.280	–	–
	omb	0.040	0.280	–	–

Note: Each *phase* variable category is encoded as a dummy variable with a value of 1 if it signifies the mentioned condition, and 0 otherwise. The minerotrophic category serves as the reference, rendering its level redundant. Marginal $r^2 = 0.64$, conditional $r^2 = 0.78$.

The model using *HUM* also explains a considerable amount of variation in $\log_{10}(K_s)$ (conditional $r^2 = 0.78$) and, as with the previous model, most of the variation is explained with the fixed-effects structure (marginal $r^2 = 0.64$). Like the preceding *LME* model, the influence of $\log_{10}$(*depth*) on the $\log_{10}(K_s)$ values varies based on the measurement locations. The model's random intercept, which fluctuates across coring locations, exhibits a variance of $\sigma^2 = 0.26$. The association between $\log_{10}$(*depth*) and $\log_{10}(K_s)$ undergoes alterations among the coring sites, characterized by a variance of $\sigma^2 = 1.38$. The coefficients of intercepts and slopes of $\log_{10}$(*depth*) for various peat cores can be found in the supplementary materials in PAPER II – Paat et al., 2022. The structure of random and fixed effects, along with the predictive capacity (marginal and conditional r_2) is analogous to the model that employs the von Post score as a predictor variable to characterize the degree of decomposition. Based on the Akaike Information Criterion, the model utilizing the *von Post* score exhibits slightly superior performance compared to the model using *HUM* (with *AIC* scores of 480 and 482, respectively) (PAPER II – Paat et al., 2022).

6.3 The performance of the predictive models

The results of the constructed predictive models indicate that measurement depth, *BD*, and the degree of decomposition, either on the von Post scale or as HUM, significantly control the $\log_{10}(K_s)$ (PAPER II – Paat et al., 2022). The fit between measured and predicted $\log_{10}(K_s)$ values is depicted in Figure 9. The overall fit across the training and testing datasets for both models is relatively good. There is a noticeable performance discrepancy over the saturated hydraulic conductivity

values, with the models being more precise for less conductive peat. Furthermore, the models' accuracy appears to be reduced for ombrotrophic/bog peat samples, which show underestimated predicted values compared to the *in-situ* measurements. Such inconsistencies could possibly be attributed to some sort of leakage of the installed piezometers during the *in-situ* conductivity tests or inaccuracies with bulk density measurements. Sampling with a Russian-type corer could introduce a slight compression, which in turn may yield higher *BD* values and, consequently, lower calculated saturated hydraulic conductivity values.

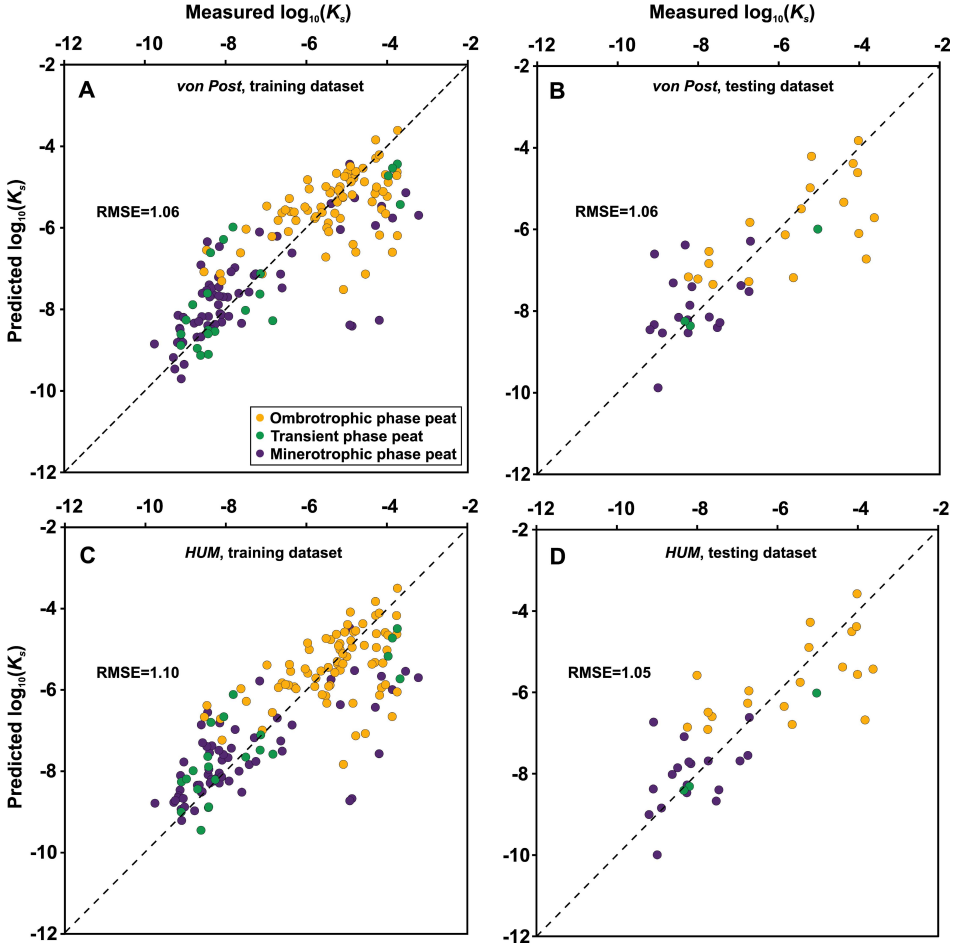

Figure 9. The performance of constructed *LME* models for $\log_{10}(K_s)$, using *von Post* score (top row) and *HUM* (bottom row) as variable for degree of decomposition. All the other independent variables are the same for both models. The left column shows the performance of the model with training and the right column with the testing dataset. Broken lines indicate a 1:1 relationship between predicted and measured values.

The results of the models indicate quite similar performance (see Figure 9 and marginal/conditional r^2 in Tables 2 and 3). Both *von Post* score and *HUM* are significant predictors of $\log_{10}(K_s)$, while the statistical models employing them show relatively similar predictive power. The finding suggests that despite *von Post* score being a more subjective and less precise measure of decomposition, it can explain the variance of $\log_{10}(K_s)$ on the same level as the laboratory-measured *HUM*. The findings of this study, alongside meta-studies such as Morris et al. (2022), reassure the usability of this parameter in further modeling endeavors, as the *von Post* score remains one of the most commonly measured proxies for characterizing peat decomposition.

The extraction of humic acids, as proposed by Blackford & Chambers (1993) has been disputed as a proxy for describing the degree of decomposition (Biester et al., 2014). However, the results and the apparent and significant correlations between *HUM* and $\log_{10}(K_s)$ (see Figure 8D and Table 1) confirm, that despite being a controversial descriptor of peat decomposition, it is associated with changes in saturated hydraulic conductivity. Nonetheless, the *von Post* score offers a distinct advantage as a predictor of K_s, as it can be rapidly assessed in situ immediately after coring, whereas determining *HUM* requires certain laboratory procedures. However, assessing humification is still more time-efficient than measuring the hydraulic conductivity of very decomposed and compacted peat layers in the field (PAPER II – Paat et al., 2022).

Both constructed models exhibit a small, yet significant location-based dependence on the modeling results, also noted by Branham & Strack. (2014) and Morris et al. (2019). Moreover, there seems to be a significant variation of sampling depth on the $\log_{10}(K_s)$ values over the different peat cores, manifested by the models' random effects structure. As mentioned before, such location-specific depth differences on saturated hydraulic conductivity are very reasonable, as each mire has a very distinct developmental history contrasted by variations in peat profiles across coring sites. The placement of various peat layers with differentiating botanical composition, *BD*, and decomposition state creates a random depth dependency altering between the measuring sites (PAPER II – Paat et al., 2022).

Such core-specific dependencies highlight the heterogeneity issue within peat when constructing general statistical models for saturated hydraulic conductivity like the ones presented here. The modeled random effects structure underscores the limitation of these models' universality, as the accuracy of mixed effects models might diminish at sites beyond those sampled in this study. Nevertheless, the overall population models, excluding the random effects (core ID and depth dependency), can still account for a significant amount of variation in $\log_{10}(K_s)$ (with marginal r^2 values of 0.66 and 0.64 for the *von Post* and *HUM* models, respectively) (PAPER II – Paat et al., 2022). These statistics suggest that the proposed models could potentially be applied to peatlands beyond those used for model construction in this study. However, it should be validated with further studies.

The constructed saturated hydraulic conductivity models are particularly necessary and advantageous for characterizing the bottommost layers of peatlands,

which are crucial for studying vertical water movement and subsurface drainage effects, as seen in Selisoo (PAPER I – Kohv et al., 2023). These statistical models include measurements up to 6.5 m in depth, making them applicable to peatlands with very thick peat deposits. Moreover, as they include extensive data from the bottommost layers of the peatlands, they are suitable for characterizing peat layers, which are the most likely to limit water flow from the surface to the underlying sediments. The application of these statistical models precludes the need for numerous *in-situ* hydraulic conductivity tests, which can be time-consuming, particularly for more decomposed and compacted peat layers. Therefore, these models should broaden the lateral and vertical extent of measurements of saturated hydraulic conductivity. Wider coverage with conductivity values is necessary for determining any pathways through which water could reach the underlying sediments faster, enhancing the effects of underground drainage, and getting a holistic idea of the peatlands' hydraulic structure. This information is necessary for the construction of more precise hydrological and hydrogeological models.

7. DETERMINATION OF VERTICAL HYDRAULIC PROPERTIES

7.1 Vertical hydraulic diffusivity

The theory proposed by Davis (1972) uses naturally occurring hydraulic pressure fluctuations in the sediment to measure the diffusion of pressure impulses within the material, through which it is possible to characterize the hydraulic properties of the medium. Analyzing the fluctuations of hydraulic pressure in Kaasiksoo and Selisoo (Figure 10) reveals that variations in atmospheric pressure are the main cause of hydraulic pressure head changes in peat. In the top 3.0 m of the peat in Kaasiksoo, there is no substantial change in the fluctuation dynamics of hydraulic pressure when comparing it to the atmospheric pressure changes. Although there is no noticeable delay in pressure changes, there is a slight decrease in amplitude. However, as the depth increases, the delay and attenuation of hydraulic pressure changes increase, coinciding with changes in botanical composition and peat properties and resulting in a decrease in the hydraulic conductivity of peat. The most significant change appears between depths of 3.2 m and 3.4 m, where the lag and attenuation of hydraulic pressure response are most prominent when compared to atmospheric pressure fluctuations (PAPER III – Paat et al., 2024).

In Selisoo, the main characteristics of the observed hydraulic pressure fluctuations are similar to those seen in Kaasiksoo. As we go deeper into the peat column, there is a clear delay and attenuation in the hydraulic pressure fluctuations compared to pressure movements in the atmosphere. A noticeable delay is already observed at 4.8 m, which is at the boundary of bog/transitional peat and fen peat, not observed at the same boundary in Kaasiksoo at 3.0 m. Similar to Kaasiksoo, there is a significant reduction in amplitude and an increase in delay when comparing head fluctuations at 5.3 m to 4.8 m, passing through the fen peat layer (PAPER III – Paat et al., 2024).

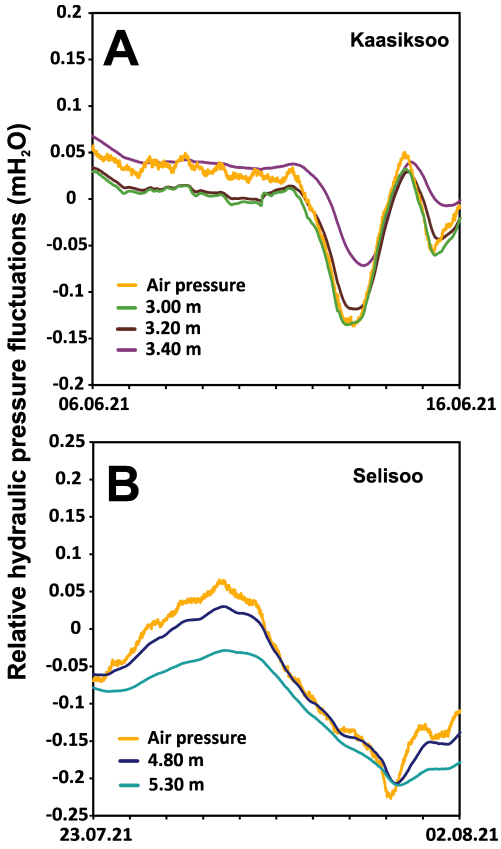

Figure 10. A ten-day-long section from time-series of the hydraulic head fluctuation t at Kaasiksoo and Selisoo, to highlight the changes in amplitude (attenuation) and time (lagged response) with increasing peat depth.

The results of the fitting process for vertical hydraulic diffusivity can be seen in Figures 11 and 12. In Kaasiksoo, the entire minerotrophic fen peat layer (3.0–3.4 m) exhibited a vertical hydraulic diffusivity value of 9.5×10^{-6} m^2s^{-1}, as depicted in Figure 11A. The associated RMSE was 0.005 m. The vertical diffusivity calculated for the shallower peat layers, spanning from the surface to a depth of 3.0 m (Figure 11D), reached the highest determined value for this parameter across all computations, measuring 4.8×10^{-3} m^2s^{-1}. The fit between measured and calculated water levels showed an RMSE of 0.010 m. At depths of 3.0–3.2 m and 3.2–3.4 m (Figures 11B and 11C), the vertical diffusivity values were determined to be 1.3×10^{-5} m^2/s^{-1} and 4.6×10^{-6} m^2s^{-1}, respectively. Remarkably, the corresponding RMSE values for these depths were 0.005 m and 0.004 m, representing the lowest among all the calculations. Moreover, the average diffusivity calculated from results covering depth intervals of 3.0–3.2 m and 3.2–3.4 m ($D_v = 8.6\times10^{-6}$ m^2 s^{-1}) shows similar outcomes to those measured across the interval of 3.0–3.4 m ($D_v = 9.5\times10^{-6}$ m^2 s^{-1}), highlighting the method's consistency and repeatability (PAPER III – Paat et al., 2024).

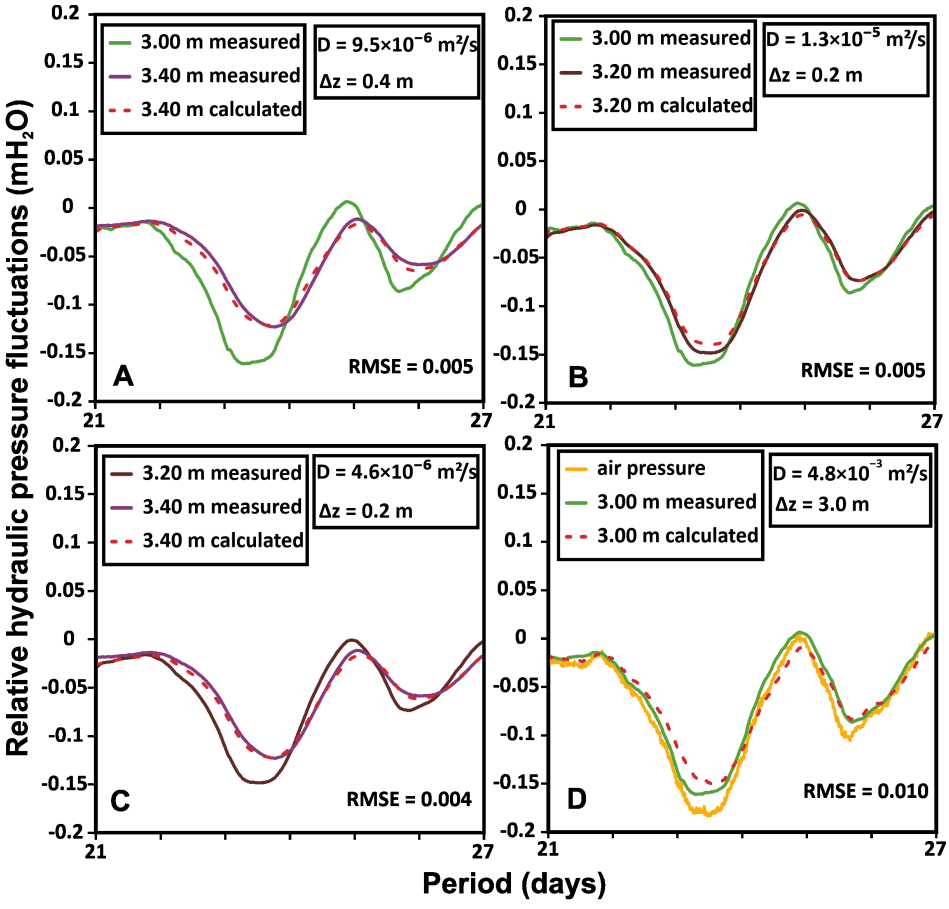

Figure 11. A ten-day-long section from the calculation results time-series of vertical hydraulic diffusivity in Kaasiksoo between different depth intervals. Figures B and C show the diffusivity fitting results over thinner intervals in fen peat at 3.0–3.2 m and 3.2–3.4 m. Figure D shows the best fit in the upper bog/transitional peat. The fit between calculated and measured values is assessed with mean root square error (*RMSE*).

In Selisoo, the calculated diffusivity of the bottommost and highly decomposed fen peat layer (4.8–5.3 m) was 1.1×10^{-5} m^2s^{-1} (Figure 12A). The comparison of measured and calculated water level fluctuations shows a relatively good fit with the *RMSE* value of 0.007 m. The vertical hydraulic diffusivity of the upper bog/transitional part (0–4.8 m) of the peat column in Selisoo (Figure 12B) was 3.7×10^{-3} m^2s^{-1}, being significantly higher than in the highly decomposed deeper peat layer. The fit between the measured and calculated time series closely resembles the previous one, with an *RMSE* of 0.006 m (PAPER III – Paat et al., 2023).

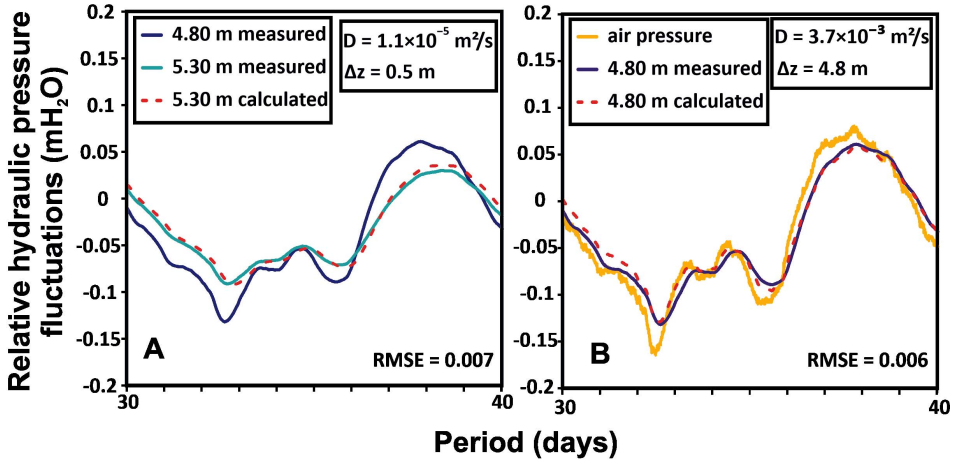

Figure 12. A ten-day-long section from the calculation results time-series of vertical hydraulic diffusivity in Selisoo between different depth intervals. Figure A describes the fitting and corresponding vertical diffusivity value in the bottommost fen peat and Figure B results in the upper bog/transitional peat portion. RMSE values describe the fit between measured and calculated values.

The computed hydraulic pressure responses, using the determined D_v values, show a relatively good fit with the *in-situ* measured pressures. The *RMSE* values are comparatively low when considering the actual hydraulic head fluctuation amplitudes observed at these study sites. However, comparing the diffusivity results with earlier studies or other methods presents a challenge due to the scarcity of conducted hydraulic diffusivity measurements in peat. The D_v values reported by Hogan et al. (2006) for a minerotrophic fen in Saskatchewan, Canada, ranging from 1.0×10^{-4} to 3.2×10^{-4} m² s^{-1}, are much higher than the results reported here. However, direct comparison may be considered unreasonable due to ambiguities in peat properties arising from differences in site locations and measurement techniques. Nevertheless, given the excellent fit between the calculated and measured values, as well as the comparable D_v values over the 3.0–3.4 m interval compared to the average over the 3.0–3.2 m and 3.2–3.4 m intervals, the proposed technique demonstrates good performance for vertical hydraulic diffusivity assessments.

7.2 Compressibility and specific storage of peat

A better comparison of the performance of the proposed methodology could be obtained from the vertical hydraulic conductivity values, which are calculated using the diffusivity and specific storage values derived from compressibility measurements. Before reaching the vertical hydraulic conductivity the coefficients of compressibility and derived specific storage values are inspected. The coefficients of compressibility determined with oedometer tests are presented in Figure 13 in unison with measured bulk density and humification values.

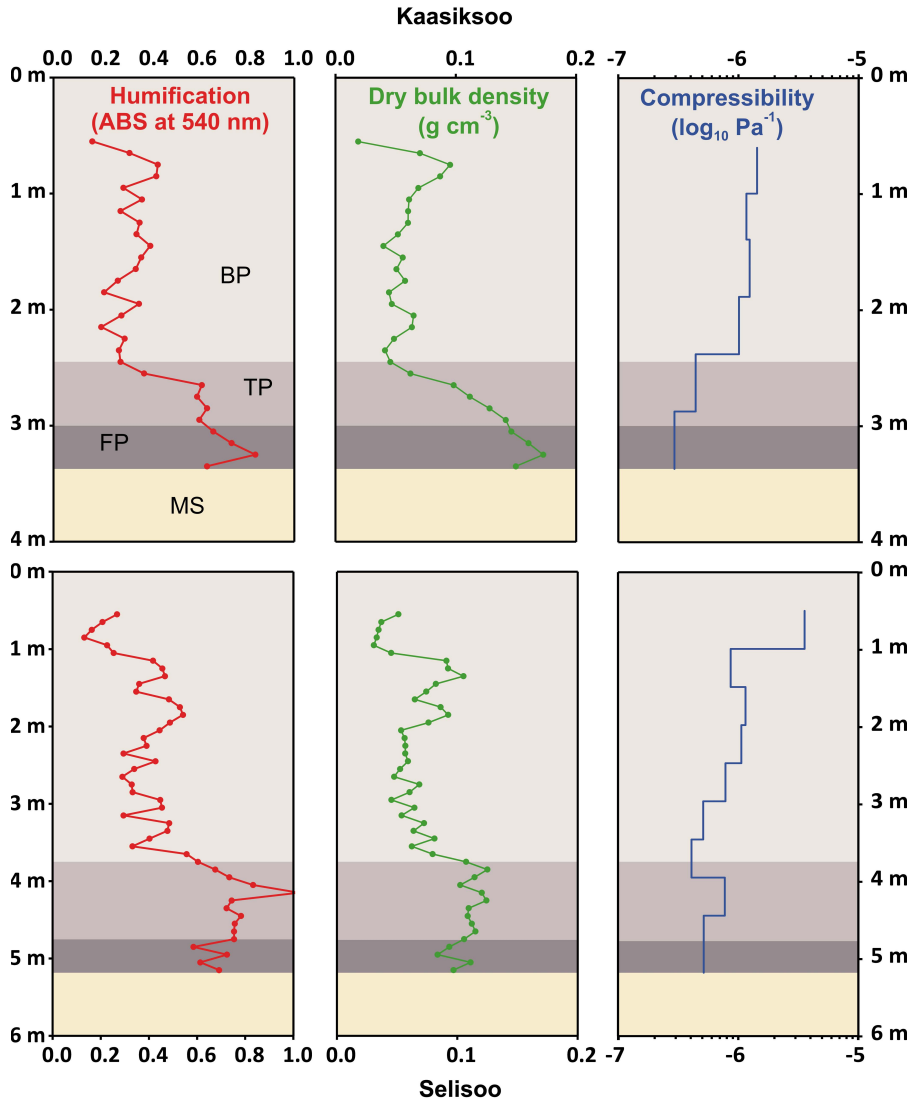

Figure 13. Coefficient of compressibility measured over 0.5 m intervals with the corresponding bulk density and humification measurements (3 cm samples) at Selisoo and Kaasiksoo. BP – bog peat, TP – transitional peat, FP – fen peat, MS – mineral sediments.

In Kaasiksoo, the compressibility coefficients ranged from 2.9×10^{-7} Pa^{-1} to 1.4×10^{-6} Pa^{-1}, showing quite stable values in the upper portion of the peat column, consisting of bog peat. The change in compressibility with depth seems to be associated with the boundaries between distinct peat types. The most pronounced shift in compressibility occurred at approximately 2.4 m depth, on the interface of bog and transitional (from rainwater-fed to groundwater-fed conditions) peat, aligning with a noticeable increase in bulk density and humification. From there, the coefficient of compressibility decreases towards the bottom of

the peat column. Looking at Figure 13, it is quite clear that compressibility values interchange with dry bulk density and humification, being higher in less dense and humified upper peat layers and lower in more compacted and humified intervals. A noteworthy observation, when comparing the two sites, is that Kaasiksoo exhibits more pronounced change in compressibility and overall peat properties among the different peat types in the peatland structure, as opposed to Selisoo (PAPER III – Paat, et al., 2024).

The compressibility values in Selisoo ranged from 4.1×10^{-7} Pa^{-1} to 3.6×10^{-6} Pa^{-1}, displaying a more noticeable variation throughout the peat column than in Kaasiksoo. Notably, at a depth of 1 m, compressibility significantly decreased due to the increased bulk density and peat humification. From 1.5 m depth onwards, compressibility continued to decrease until reaching the transitional section of the peat column, where bog plant species shifted to fen species. Unlike in Kaasiksoo, transitional and fen peat in Selisoo exhibited higher compressibility values than in the bottommost bog peat layers. These variations in compressibility with depth between the two sites closely mirrored the measured dry bulk density. In Selisoo, bulk density among different peat layers appeared less variable than in Kaasiksoo, where it sharply increased during the transition from bog peat to fen peat (PAPER III – Paat et al., 2024)

Table 4. Hydraulic diffusivity (K_v/S_s), compressibility (α), and derived vertical hydraulic conductivity (K_v) values.

Site	Interval (m)	K_v/S_s ($m^2\ s^{-1}$)	α (Pa^{-1})	S_s (m^{-1})	K_v ($m\ s^{-1}$)
KAASIK-SOO	0–3.0	4.8×10^{-3}	$1.0\times10^{-6*}$	$1.0\times10^{-2*}$	4.9×10^{-5}
	3.0–3.2	1.3×10^{-5}	2.9×10^{-7}	2.9×10^{-3}	3.6×10^{-8}
	3.2–3.4	4.6×10^{-6}	2.9×10^{-7}	2.9×10^{-3}	1.3×10^{-8}
	3.0–3.4	9.5×10^{-6}	2.9×10^{-7}	2.9×10^{-3}	2.7×10^{-8}
SELISOO	0–4.8	3.7×10^{-3}	$1.1\times10^{-6*}$	$1.1\times10^{-2*}$	4.1×10^{-5}
	4.8–5.3	1.1×10^{-5}	5.2×10^{-7}	5.1×10^{-3}	5.6×10^{-8}

* The **α** and **S_s** values for the upper bog and transitional peat layers (0–4.8 m in SELI and 0–3.0 m KAS) are taken as a weighted average over all the oedometer test results in the interval.

The derived specific storage values from the measured compressibility coefficients are seen in Table 4 alongside the corresponding calculated vertical hydraulic conductivity values. The specific storage values ranged from 2.9×10^{-3} m^{-1} to 1.1×10^{-2} m^{-1} at the measuring sites, being higher in shallower peat layers and lower in deeper layers, as the storage properties are interlinked with the compressibility of peat.

7.3 Vertical hydraulic conductivity

In order to evaluate the effectiveness of the proposed method and confirm the accuracy of the measured vertical diffusivity and compressibility/specific storage values, a comparison of conductivity values is presented (Figure 14). From there, the values for the K_v results, obtained using the proposed method in question, and the conductivity values, obtained *in-situ* and in laboratory with oedometer cell permeability tests, could be seen. The *in-situ* measurements in Kaasiksoo have been conducted using falling head slug-tests and BAT-permeameters, which results are reported in PAPER II (Paat et al., 2022). The on-site measurements in Selisoo have also been done using BAT-permeameters, but data has not been previously published. More precise values for K_v can be found in Table 4. In Kaasiksoo, the K_v values determined for the bottommost fen peat appear to be significantly higher than those measured in laboratory conditions, with K_v at 2.7×10^{-8} m s^{-1} compared to K_{oed} at 3.5×10^{-9} m s^{-1}, and two orders of magnitude higher than the K_s of 7.9×10^{-10} m s^{-1} measured with a BAT- permeameter at a depth of 3.3 meters. Meanwhile, in Selisoo, the determined K_v value of 5.6×10^{-8} m s^{-1} for the fen peat aligns more closely with K_{oed} (3.2×10^{-7} m s^{-1}) and the *in-situ* measured K_s (8.1×10^{-8} m s^{-1}). Notably, for both sites, the K_v values in the upper bog/transitional section appear to be significantly elevated compared to the other *in-situ* and laboratory-measured hydraulic conductivities (PAPER III – Paat et al., 2024).

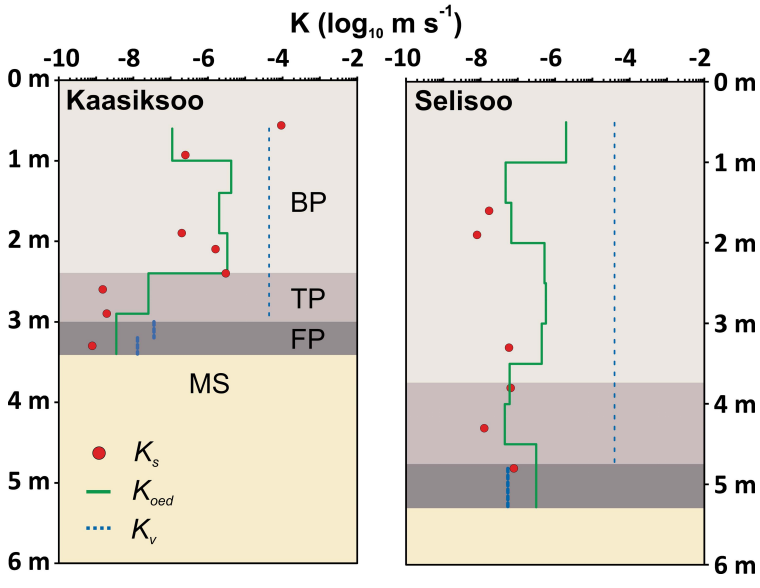

Figure 14. Comparison of the vertical hydraulic conductivity. K_v – values calculated through derived D_v and S_s values; K_{oed} – laboratory falling head oedometer permeability tests; K_s – saturated hydraulic conductivity tests (conducted by Paat et al., 2022 in Kaasiksoo and previously unpublished measurements in Selisoo using the same *in-situ* methods). BP – bog peat; TP – transitional peat; FP – fen peat; MS – underlying mineral sediments (PAPER III – Paat et al., 2024).

While it seems that the K_v values are contrasting from the results of more commonly used methods, some considerations should be acquainted over this comparison. Firstly, the seemingly lower K_s values in Kaasiksoo, compared to K_v could be attributed to the smearing or clogging of the BAT-permeameter (Torstensson, 1984) filter tip during the installation. Such an effect concerning this testing apparatus has been reported by e.g., Arulrajah et al. (2006) and Bo et al. (2014) in clayey sediments (PAPER II – Paat et al., 2022). The bottommost layer in Kaasiksoo also consists of highly decomposed and thus texturally amorphous and fine particle peat sediments, which could clog up the porous membrane of the BAT filter tip and thus give lower conductivity values than expected.

Some discussions should also be cast on K_s as a parameter to be used in characterizing and paralleling the vertical water movement. The results of the *in-situ* conducted piezometer or slug-tests and permeameter tests are generally considered to describe the water movement in the horizontal rather than in the vertical direction (Surridge et al., 2005). Many authors (e.g., Beckwith et al., 2003; Rosa & Larocque, 2008; Surridge et al., 2005) have shown that peat is an anisotropic medium and thus should exhibit preferential flow paths. Therefore, any direct comparisons between the saturated hydraulic conductivity (K_s) and vertical conductivity (K_v) should be approached with caution.

Moreover, K_v is measured over a larger interval and characterized over different peat intervals, compared to the "point" measurements of K_s (3 cm long filters for BAT-permeameter), conducted in more homogenous conditions. The same concerns arise while comparing K_v results with K_{oed}, as they characterize hydraulic conductivities over entirely different intervals, while also minding that the peat samples experienced disturbance during initial collection and placement to the oedometer ring.

Secondly, it is crucial to account for the potential presence of conduits connecting the buried pressure sensors measuring hydraulic heads. These conduits might accelerate the transmission of pressure change impulses (Seo, 2001) reaching deeper measuring depths, potentially resulting in seemingly inflated values of vertical hydraulic diffusivity. Improper installation practices, like insufficient sealing of pressure transducers, the proximity of neighboring monitoring wells penetrating the studied peat layers, and for raised bogs even the nearby bog pools intersecting to the same peat layers, could all contribute to the formation of such conduits. Even the insertion of several buried pressure transducers next to each other could enhance the connectivity of deeper-lying sensors to the hydraulic head fluctuations happening at the peat surface.

Also worth noting is the evaluation of specific storage, which values have been derived from a harmonic average value of compressibility over all the measurements included in the observed interval. For the bottommost fen peat intervals, the compressibility measurements cover more or less the same intervals for which the vertical hydraulic diffusivity has been calculated. It should also be considered that oedometer tests are one-dimensional in nature (compression happens only in one direction) (Price et al., 2005). On-site measured compressibility would be preferable as it would provide a measure for real unconstrained

(three-dimensional) compression. Using *InSAR* (Alshammari et al., 2020; Tampuu, Praks, Uiboupin, & Kull, 2020) or anchored elevation sensor rods (Price, 2003) to measure peat subsidence concurrently with hydraulic pressure measurements could provide a way of measuring *in-situ* peat compressibility (PAPER III – Paat et al., 2024).

In conclusion, it is difficult to validate the vertical hydraulic conductivity results, as this methodology has not been utilized in peat soils before, and thus, there is a lack of comparable measurements. However, considering the above-mentioned, the comparisons offered here still show a relatively close resemblance to conductivity values, in particular for the deeper and more decomposed peat intervals. It is somewhat unclear whether the measurements of K_v over the upper bog/transitional peat layers are representative. The higher vertical hydraulic conductivity of bog peat could potentially violate the underlying one-dimensional flow assumptions of this approach (Davis, 1972), as it was originally intended and used in semi-permeable aquitards. It is exemplified by the minimal delays and attenuations of pressure impulses between the installed pressure transducers (see Figure 10) in the upper, younger, and less decomposed parts of the cross-sections. However, even without the contrasting impulse diffusion, the vertical hydraulic diffusivity estimation with this technique seems feasible. That said, using hydraulic head fluctuations for measuring vertical diffusivity in less decomposed and dense peat layers should be further investigated to better comprehend the limitations of this method (PAPER III – Paat et al., 2024).

7.4 Benefits of such measuring technique

The data provided here confirms the potential of using naturally occurring hydraulic pressure fluctuations to assess the vertical hydraulic parameters of peat. The attenuation and delay of the hydraulic pressure fluctuation amplitudes are seen passing through peat layers with different physical properties. Even if the validity of the results is difficult to assess, due to inadequacies of similar and directly comparable data, the method itself seems to provide reasonable and logical outcomes. As such approach has not been used or, at least, widely recognized in peatland hydrology studies, it is imperative to conduct further research employing such technique to provide more data and validate its usage in other peatlands in different climatic zones. Further conductivity measurements in less decomposed and more conductive peat layers are certainly important to understand the limitations of the method better.

The merit of this method is mostly connected with offering more comprehensive information about the water movement in peatlands, particularly concerning their hydrogeological connectivity to underlying geological formations and water movement between them. The significance of the acquired data especially arises while assessing the effects of lowering hydraulic heads with drainage in the underlying aquifers on peatlands (Balliston & Price, 2023; Kohv et al., 2023; Whittington & Price, 2013). In the circumstances where the vertical hydraulic

gradients between the water level in peatlands and the underlying mineral aquifer are rising (PAPER I – Kohv et al., 2023), the conductivity, in conjunction with a thickness of peat itself has a defining role in restricting the downward flow of water. This measuring technique creates a relatively simple way to estimate the vertical conductivities of deeper-lying and far less accessible peat intervals, significantly understudied and overlooked.

Another benefit of using this methodology lies in its capacity to provide valuable insights into the bulk-saturated hydraulic conductivity of peat over larger intervals. Unlike commonly reported conductivity tests such as slug-tests or permeameter tests, which typically focus on water flow over very small intervals and in close proximity to the measuring apparatus (Glaser et al., 2021), this method offers a broader perspective. By encompassing larger volumes of peat, it reduces susceptibility to scale dependency, a significant concern due to the inherent heterogeneity of peat (Beckwith et al., 2003; McCarter et al., 2020). Consequently, obtaining conductivity values over larger intervals enhances the accuracy of hydraulic data crucial for developing peatland water flow models (PAPER III – Paat et al., 2024).

8. CONCLUSIONS

The aim of this thesis was twofold. Firstly, it aimed to analyze long-term hydraulic head data from a raised bog in northeastern Estonia, situated near an active oil-shale mine, to confirm the effects of underground drainage on the peatland. Secondly, it aimed to provide insights into the hydraulic and physical properties of peat considering such drainage influences, and to offer tools and methods necessary for conducting future hydrological studies in the region and possibly in other hemi-boreal peatlands, particularly regarding vertical water movement in peatlands during underground drainage.

The main conclusions of the study are:

1) Underground, mining-induced drainage lowers hydraulic heads in regional aquifers, affecting the hydrology of nearby Selisoo raised bog. The overlying regional aquitards are insufficient to protect the topmost Quaternary aquifer from deeper drainage influences.
2) Hydraulic heads are significantly lowered in the mineral sediments beneath the peat, extending under the bog centers. Decreasing hydraulic heads are observed within the peat, especially near bog margins where peat is thinner, and in the surrounding drained bog forests. The two bog centers appear to remain intact due to thicker peat limiting water flow from the peatland surface to the underlying drained mineral sediments.
3) The spatial integrity and overall hydraulic conductivity of peat are crucial for determining water movement through peat during underground drainage and thus making them the key elements to ascertain the persistence of the peatlands in such hydrogeological conditions.
4) The minerotrophic fen peat with transitional peat, separating peatlands from the underlying mineral sediments, exhibit the lowest saturated hydraulic conductivity values. This confirms the significance of the bottommost peat layers in isolating and limiting water flow from the peatland surface to the underlying sediments during underground drainage.
5) The saturated hydraulic conductivity is negatively correlated with commonly measured peat characteristics such as measurement depth, dry bulk density, von Post score, and humification. Statistical models constructed using these characteristics can relatively accurately predict saturated hydraulic conductivity. However, it is important to consider location-based dependencies, transpired with this study, when using these models.
6) There is a noticeable diffusion of hydraulic pressure impulses occurring in peat. The main driver of pressure changes at the surface of peat is the fluctuations in atmospheric pressure. The attenuation and delay of pressure changes happening at the peat surface increase with depth into the peatland. Measuring hydraulic pressure at two different depths allows the calculation of vertical hydraulic diffusivity of peat between the two sensors.

7) The combination of hydraulic diffusivity values with the specific storage of peat, derived from its compressibility, yields vertical hydraulic conductivity results for the bottommost, more humified, and dense peat layers that are comparable to those obtained using more widely used methods. While compressibility measurements with standard laboratory oedometer tests could be used for this purpose, it would be advisable to determine suitable *in-situ* methods for characterizing this parameter in future studies.

The findings presented here provide invaluable insights into the hydraulic structure of hemi-boreal peatlands in northeastern Estonia and shed light on the effects of underground drainage on these ecosystems. The models and methods outlined in this study are practical and essential for future research on peatland hydrology in this region, as they contribute to the construction of more precise hydrological and hydrogeological models. Moreover, these approaches are also encouraged to be used in other hemi-boreal peatlands and regions worldwide for testing and improvement purposes.

REFERENCES

Alshammari, L., Boyd, D. S., Sowter, A., Marshall, C., Andersen, R., Gilbert, P., … Large, D. J. (2020). Use of Surface Motion Characteristics Determined by InSAR to Assess Peatland Condition. *Journal of Geophysical Research: Biogeosciences*, *125*(1). https://doi.org/10.1029/2018JG004953

Arulrajah, A., Nikraz, H., & Bo, M. W. (2006). In Situ Pore Water Pressure Dissipation Testing of Marine Clay under Reclamation Fills. *Geotechnical and Geological Engineering*, *24*(1), 29–43. https://doi.org/10.1007/s10706-004-1807-x

Baird, A. J., Surridge, B. W. J., & Money, R. P. (2004). An assessment of the piezometer method for measuring the hydraulic conductivity of a Cladium mariscus – Phragmites australis root mat in a Norfolk (UK) fen. *Hydrological Processes*, *18*(2), 275–291. https://doi.org/10.1002/hyp.1375

Balliston, N. E., & Price, J. S. (2023). Aquifer depressurization and water table lowering induces landscape scale subsidence and hydrophysical change in peatlands of the Hudson Bay Lowlands. *Science of the Total Environment*, *855*(May 2022), 158837. https://doi.org/10.1016/j.scitotenv.2022.158837

Barton, K. (2020). MuMIn: Multi-Model Inference. Retrieved from https://cran.r-project.org/package=MuMIn

Bauert, H., & Kattai, V. (1997). Kukersite oil shale. In A. Raukas & A. Teedumäe (Eds.), *Geology and Mineral Resources of Estonia*. Tallinn: Estonian Academy Publishers.

Beckwith, C. W., Baird, A. J., & Heathwaite, A. L. (2003). Anisotropy and depth-related heterogeneity of hydraulic conductivity in a bog peat. I: Laboratory measurements. *Hydrological Processes*, *17*(1), 89–101. https://doi.org/10.1002/hyp.1116

Biester, H., Knorr, K. H., Schellekens, J., Basler, A., & Hermanns, Y. M. (2014). Comparison of different methods to determine the degree of peat decomposition in peat bogs. *Biogeosciences*, *11*(10), 2691–2707. https://doi.org/10.5194/bg-11-2691-2014

Blackford, J. J., & Chambers, F. M. (1993). Determining the degree of peat decomposition for peat-based palaeoclimatic studies. *International Peat Journal*, *5*, 7–24.

Bo, M. W., Arulrajah, A., Leong, M., Horpibulsuk, S., & Disfani, M. M. (2014). Evaluating the in-situ hydraulic conductivity of soft soil under land reclamation fills with the BAT permeameter. *Engineering Geology*, *168*, 98–103. https://doi.org/10.1016/j.enggeo.2013.11.001

Branham, J. E., & Strack, M. (2014). Saturated hydraulic conductivity in Sphagnum-dominated peatlands: Do microforms matter? *Hydrological Processes*. https://doi.org/10.1002/hyp.10228

Bromley, J., Robinson, M., & Barker, J. A. (2004). Scale-dependency of hydraulic conductivity: an example from Thorne Moor, a raised mire in South Yorkshire, UK. *Hydrological Processes*, *18*(5), 973–985. https://doi.org/10.1002/hyp.1341

Carslaw, D. C., & Ropkins, K. (2012). openair – An R package for air quality data analysis. *Environmental Modelling & Software*, *27–28*, 52–61. https://doi.org/10.1016/j.envsoft.2011.09.008

Chambers, F. M., Beilman, D. W., & Yu, Z. (2011). Methods for determining peat humification and for quantifying peat bulk density , organic matter and carbon content for palaeostudies of climate and peatland carbon dynamics. *Mires and Peat*, *7*(September 2016), 1–10.

Chason, D. B., & Siegel, D. I. (1986). Hydraulic conductivity and related physical properties of peat, Lost River peatland northern Minnesota. *Soil Science*, *142*(2), 91–99. https://doi.org/10.1097/00010694-198608000-00005

Clevend, R. B., Cleveland, W. S., McRae, J. E., & Terpenning, I. (1990). STL: A Seasonal-Trend Decomposition Procedure Based on Loess. *Jornal of Official Statistics*, *6*(1), 3–73. https://doi.org/10.1007/978-1-4613-4499-5_24

Clymo, R. S. (2004). Hydraulic conductivity of peat at Ellergower Moss, Scotland. *Hydrological Processes*, *18*(2), 261–274. https://doi.org/10.1002/hyp.1374

Comas, X., Slater, L., & Reeve, A. S. (2011). Pool patterning in a northern peatland: Geophysical evidence for the role of postglacial landforms. *Journal of Hydrology*, *399*(3–4), 173–184. https://doi.org/10.1016/j.jhydrol.2010.12.031

Davis, R. W. (1972). Use of naturally occurring phenomena to study hydraulic diffusivities of aquitards. *Water Resources Research*, *8*(2), 500–507. https://doi.org/10.1029/WR008i002p00500

Dong, L., Chen, J., Fu, C., & Jiang, H. (2012). Analysis of groundwater-level fluctuation in a coastal confined aquifer induced by sea-level variation. *Hydrogeology Journal*, *20*(4), 719–726. https://doi.org/10.1007/s10040-012-0838-2

FAO. (2020). *Peatlands mapping and monitoring – Recommendations and technical overview*. Rome: Food and Agriculture Organization of the United Nations. https://doi.org/10.4060/ca8200en

Fetter, C. W. (2001). *Applied Hydrogeology* (4th ed.). New Jersey: Prentice-Hall Inc. *Geotechnical investigation and testing – Laboratory testing of soil – Part 5: Incremental loading oedometer test (ISO 17892-5:2017)*. (2017).

Geotechnical investigation and testing – Laboratory testing of soil – Part 11: Permeability tests (ISO 17892-11:2019). (2019). International Organizationfor Standardization.

Glaser, P. H., Rhoades, J., & Reeve, A. S. (2021). The hydraulic conductivity of peat with respect to scaling, botanical composition, and greenhouse gas transport: Mini-aquifer tests from the Red Lake Peatland, Minnesota. *Journal of Hydrology*, *596*(October 2020), 125686. https://doi.org/10.1016/j.jhydrol.2020.125686

Gorham, E. (1991). Northern Peatlands: Role in the Carbon Cycle and Probable Responses to Climatic Warming. *Ecological Applications*, *1*(2), 182–195. https://doi.org/10.2307/1941811

Helsel, D. R., Hirsch, R. M., Ryberg, K. R., Archfield, S. A., & Gilroy, E. J. (2020). Statistical Methods in Water Resources Techniques and Methods 4 – A3. *USGS Techniques and Methods*.

Hiiemaa, H., Mustasaar, M., Kohv, M., Hang, T., Jõeleht, A., Lasberg, K., & Kalm, V. (2014). Geological settings of the protected Selisoo mire (northeastern Estonia) threatened by oil shale mining. *Estonian Journal of Earth Sciences*, *63*(2), 97. https://doi.org/10.3176/earth.2014.09

Hogan, J. M., van der Kamp, G., Barbour, S. L., & Schmidt, R. (2006). Field methods for measuring hydraulic properties of peat deposits. *Hydrological Processes*, *20*(17), 3635–3649. https://doi.org/10.1002/hyp.6379

Honaker, J., King, G., & Blackwell, M. (2011). Amelia II: A program for Missing Data. *Journal of Statistical Software*, *45*(7).

Hvorslev, M. J. (1951). Time Lag and Soil Permeability in Ground-Water Observations. *Waterways Experimental Station Bulletin 36*, 1–50.

Joosten, H., & Clarke, D. (2002). *Wise use of mires and peatlands – Background and principles including a framework for decision-making*. *International Mire Conservation Group and International Peat Society*. Retrieved from http://www.gret-perg.ulaval.ca/fileadmin/fichiers/fichiersGRET/pdf/Doc_generale/WUMP_Wise_Use_of_Mires_and_Peatlands_book.pdf

Joosten, Hans. (2009a). Human impacts: Farming, fire, forestry and fuel. In E. Maltby & T. Barker (Eds.), *The Wetlands Handbook* (pp. 698–718). Chichester: Wiley-Blackwell.

Joosten, Hans. (2009b). *The Global Peatland CO2 Picture: Peatland status and drainage related emissions in all the countries of the world*. *Wetlands International*. Wetlands International. Retrieved from http://www.wetlands.org/LinkClick.aspx?fileticket=fcVE4EMiG%2Fw%3D&tabid=56

Kattai, V., Saadre, T., & Savitski, L. (2000). *Estonian oil-shale: Geology, resources and mining conditions (in estonian)*. Tallinn.

Kohv, M., Paat, R., Lõhmus, A., & Jõeleht, A. (2023). Underground mining magnifies drought impacts in an adjacent protected raised bog. *Ecohydrology*, (January). https://doi.org/10.1002/eco.2594

Koppel, K., Michelson, A., Tamm, I., Metsur, M., Murd, M., Väli, E., & Reinsalu, E. (2018). *Põlevkivi kaevandamise eelispiirkondade määramine looduskeskkonna ja majanduslike tingimuste põhjal*. Tallinn.

Kværner, J., & Snilsberg, P. (2011). Groundwater hydrology of boreal peatlands above a bedrock tunnel – Drainage impacts and surface water groundwater interactions. *Journal of Hydrology*, *403*(3–4), 278–291. https://doi.org/10.1016/j.jhydrol.2011.04.006

Liu, H., & Lennartz, B. (2019). Hydraulic properties of peat soils along a bulk density gradient – A meta study. *Hydrological Processes*, *33*(1), 101–114. https://doi.org/10.1002/hyp.13314

Marandi, A., Karro, E., Polikarpus, M., Jõeleht, A., Kohv, M., Hang, T., & Hiiemaa, H. (2013). Simulation of the hydrogeologic effects of oil-shale mining on the neighbouring wetland water balance: case study in north-eastern Estonia. *Hydrogeology Journal*, *21*(7), 1581–1591. https://doi.org/10.1007/s10040-013-1032-x

Marandi, A., Veinla, H., & Karro, E. (2014). Legal aspects related to the effect of underground mining close to the site entered into the list of potential Natura 2000 network areas. *Environmental Science and Policy*, *38*, 217–224. https://doi.org/10.1016/j.envsci.2014.01.003

Masing, V. (1984). Estonian bogs: plant cover, succession and classification. In P. . Moore (Ed.), *European mires* (pp. 119–148). London: Academic Press.

McCarter, C. P. R., Rezanezhad, F., Quinton, W. L., Gharedaghloo, B., Lennartz, B., Price, J., … Van Cappellen, P. (2020, August 1). Pore-scale controls on hydrological and geochemical processes in peat: Implications on interacting processes. *Earth-Science Reviews*. Elsevier B.V. https://doi.org/10.1016/j.earscirev.2020.103227

Morris, P. J., Davies, M. L., Baird, A. J., Balliston, N., Bourgault, M. A., Clymo, R. S., … Wilkinson, S. L. (2022). Saturated Hydraulic Conductivity in Northern Peats Inferred From Other Measurements. *Water Resources Research*, *58*(11). https://doi.org/10.1029/2022WR033181

Morris, Paul J., Baird, A. J., & Belyea, L. R. (2015). Bridging the gap between models and measurements of peat hydraulic conductivity. *Water Resources Research*, *51*(7), 5353–5364. https://doi.org/10.1002/2015WR017264

Morris, Paul J., Baird, A. J., Eades, P. A., & Surridge, B. W. J. (2019). Controls on Near-Surface Hydraulic Conductivity in a Raised Bog. *Water Resources Research*, *55*(2), 1531–1543. https://doi.org/10.1029/2018WR024566

Nakagawa, S., & Schielzeth, H. (2013). A general and simple method for obtaining R2 from generalized linear mixed-effects models. *Methods in Ecology and Evolution*, *4*(2), 133–142. https://doi.org/10.1111/j.2041-210x.2012.00261.x

Nichols, J. E., & Peteet, D. M. (2019). Rapid expansion of northern peatlands and doubled estimate of carbon storage. *Nature Geoscience*, *12*(11), 917–921. https://doi.org/10.1038/s41561-019-0454-z

Orru, M., Vaizene, V., Pastarus, J. R., Systra, Y., & Valgma, I. (2013). Possibilities of oil shale mining under the Selisoo mire of the Estonia oil shale deposit. *Environmental Earth Sciences*, *70*(7), 3311–3321. https://doi.org/10.1007/s12665-013-2396-x

Paal, J, Ilomets, M., Fremstad, E., Moen, A., Børset, E., Kuusemets, V., … Leibak, E. (1998). Estonian wetlands inventory 1997 : publication of the Project "Estonian Wetlands Conservation and Management." Tartu: Eesti Loodusfoto.

Paal, Jaanus, & Leibak, E. (2011). Estonian Mires: Inventory of Habitats. Publication of the Project 'Estonian Mires Inventory Completion for Maintaining Biodiversity.' Tartu: Eestimaa Looduse Fond.

Paat, R., Kohv, M., & Jõeleht, A. (2022). Saturated hydraulic conductivity of boreal peat and its relationships with peat properties and sampling depth. *Hydrological Processes*, *36*(2), 1–12. https://doi.org/10.1002/hyp.14487

Paat, R., Jõeleht, A., Sarap, G. S., & Kohv, M. (2024). Determining peat's vertical hydraulic diffusivity and hydraulic conductivity from naturally occurring hydraulic pressure fluctuations measured at various depths. *Hydrological Processes*, *38*(7), 1–14. https://doi.org/10.1002/hyp.15236

Paavilainen, E., & Päivänen, J. (1995). *Peatland Forestry* (Vol. 111). Berlin, Heidelberg: Springer Berlin Heidelberg. https://doi.org/10.1007/978-3-662-03125-4

Päivänen, J. (1973). Hydraulic conductivity and water retention in peat soils. *Acta Forestalia Fennica*, *129*. Retrieved from https://www.silvafennica.fi/pdf/article7563.pdf

Perens, R., & Vallner, L. (1997). *Geology and Mineral Resources of Estonia*. (A. Raukas & A. Teedumäe, Eds.). Tallinn: Estonian Academy Publishers.

Pintero, J., Bates, D., DebRoy, S., Sakar, D., & R Core Team. (2020). nlme: Linear and Nonlinear Mixed Effects Models. Retrieved from https://cran.r-project.org/package=nlme

Price, J. S. (2003). Role and character of seasonal peat soil deformation on the hydrology of undisturbed and cutover peatlands. *Water Resources Research*, *39*(9), 1–10. https://doi.org/10.1029/2002WR001302

Price, J. S., Cagampan, J., & Kellner, E. (2005). Assessment of peat compressibility: Is there an easy way? *Hydrological Processes*, *19*(17), 3469–3475. https://doi.org/10.1002/hyp.6068

Puura, V., & Vaher, R. (1997). Cover structure. In A. Raukas & A. Teedumäe (Eds.), *Geology and Mineral Resources of Estonia* (p. 436). Tallinn: Estonian Academy Publishers.

R Core Team. (2020). R: A Language and Enviroment for Statistical Computing. Vienna, Austria: R Foundation for Statistical Computing. Retrieved from https://www.r-project.org/

Raukas, A., & Kajak, K. (1997). Quaternary cover. In A. Raukas & A. Teedumäe (Eds.), *Geology and Mineral Resources of Estonia* (p. 436). Tallinn: Estonian Academy Publishers.

Raukas, A., & Punning, J. M. (2009). Environmental problems in the Estonian oil shale industry. *Energy and Environmental Science*, *2*(7), 723–728. https://doi.org/10.1039/b819315k

Regan, S., Flynn, R., Gill, L., Naughton, O., & Johnston, P. (2019). Impacts of Groundwater Drainage on Peatland Subsidence and Its Ecological Implications on an Atlantic Raised Bog. *Water Resources Research*, *55*(7), 6153–6168. https://doi.org/10.1029/2019WR024937

Rezanezhad, F., Quinton, W. L., Price, J. S., Elliot, T. R., Elrick, D., & Shook, K. R. (2010). Influence of pore size and geometry on peat unsaturated hydraulic conductivity computed from 3D computed tomography image analysis. *Hydrological Processes*, *24*(21), 2983–2994. https://doi.org/10.1002/hyp.7709

Rezanezhad, F., Quinton, W. L., Price, J. S., Elrick, D., Elliot, T. R., & Heck, R. J. (2009). Examining the effect of pore size distribution and shape on flow through unsaturated peat using computed tomography. *Hydrology and Earth System Sciences*, *13*(10), 1993–2002. https://doi.org/10.5194/hess-13-1993-2009

Roosalu, R. (2023). *Consolidated Balance of Mineral Resources of the Republic of Estonia for the Year 2023*. Tallinn.

Rosa, E., & Larocque, M. (2008). Investigating peat hydrological properties using field and laboratory methods: Application to the Lanoraie peatland complex (southern Quebec, Canada). *Hydrological Processes*, *22*(12), 1866–1875. https://doi.org/10.1002/hyp.6771

Rydin, H., & Jeglum, J. K. (2006). *The Biology of Peatlands*. Oxford University Press. https://doi.org/10.1093/acprof:oso/9780198528722.001.0001

Surridge, B. W. J., Baird, A. J., & Heathwaite, A. L. (2005). Evaluating the quality of hydraulic conductivity estimates from piezometer slug tests in peat. *Hydrological Processes*, *19*(6), 1227–1244. https://doi.org/10.1002/hyp.5653

Tampuu, T., Praks, J., Uiboupin, R., & Kull, A. (2020). Long Term Interferometric Temporal Coherence and DInSAR Phase in Northern Peatlands. *Remote Sensing*, *12*(10), 1566. https://doi.org/10.3390/rs12101566

Thornthwaite, C. W. (1948). An Approach toward a Rational Classification of Climate. *Geographical Review*, *38*(1), 55. https://doi.org/10.2307/210739

Torstensson, B.-A. (1984). A New System for Ground Water Monitoring. *Groundwater Monitoring & Remediation*, *4*(4), 131–138. https://doi.org/10.1111/j.1745-6592.1984.tb00904.x

UNEP. (2022). *Global Peatlands Assessment – The State of the World's Peatlands: Evidence for action toward the conservation, restoration, and sustainable management of peatlands*. Nairobi.

Vicente-Serrano, S. M., Beguería, S., & López-Moreno, J. I. (2010). A Multiscalar Drought Index Sensitive to Global Warming: The Standardized Precipitation Evapotranspiration Index. *Journal of Climate*, *23*(7), 1696–1718. https://doi.org/10.1175/2009JCLI2909.1

Whittington, P., & Price, J. S. (2013). Effect of mine dewatering on the peatlands of the James Bay Lowland: The role of marine sediments on mitigating peatland drainage. *Hydrological Processes*, *27*(13), 1845–1853. https://doi.org/10.1002/hyp.9858

Xia, Y. Y., Li, H. C., Zhao, H. Y., Wang, S. Z., Li, H. K., & Yan, H. (2019). Peatland development and environmental change during the past 1600 years in Baijianghe Mire of Changbai Mountains, China. *Quaternary International*, *528*(February), 41–52. https://doi.org/10.1016/j.quaint.2019.03.012

Yu, Z., Loisel, J., Brosseau, D. P., Beilman, D. W., & Hunt, S. J. (2010). Global peatland dynamics since the Last Glacial Maximum. *Geophysical Research Letters*, *37*(13), 1–5. https://doi.org/10.1029/2010GL043584

Zeileis, A., Leisch, F., Hornik, K., & Kleiber, C. (2002). strucchange : An R Package for Testing for Structural Change in Linear Regression Models. *Journal of Statistical Software*, *7*(2). https://doi.org/10.18637/jss.v007.i02

Zuur, A. F., Ieno, E. N., Walker, N., Saveliev, A. A., & Smith, G. M. (2009). *Mixed effects models and extensions in ecology with R. Smart Society: A Sociological Perspective on Smart Living*. New York, NY: Springer New York. https://doi.org/10.1007/978-0-387-87458-6

SUMMARY IN ESTONIAN

Põhja- ja pinnavee vastasmõjud Kirde-Eesti turbaaladel

Sood ja turbaalad on väga tähtsad ökosüsteemid. Maailma mõistes täidavad need mitmeid väga olulisi rolle, olles vajalikud ja kohati lausa endeemsed elupaigad erinevatele looma- ja taimeliikidele, pinnase süsiniku hoidlad ja maastike veerežiimi regulaatorid. Nimetatud põhjused näitavad väga selgelt, miks on need elukohatüübid meile tähtsad ja miks on sood sisse kirjutatud paljudesse looduskaitselistesse raamdirektiividesse, nagu näiteks Ramsar ja Natura 2000. Samas tuleb nentida, et viimase sajandi jooksul on soode pindala maailmas oluliselt vähenenud ja et see väheneb kiirusega, mis ületab nende tekkekiirust kogu Holotseeni jooksul. Soode pindala drastilist vähenemist mõjutab inimtegevus, ennekõike põllumajandus, metsandus ja turba tootmine. Nimetatud tegevuste tõttu on paljud endised sood kuivendatud ning need on muutunud pikaajaliselt süsinikku siduvatest ökosüsteemidest seda vabastavaks, mis tänapäevases maailmas on suur probleem.

Ka Eesti maastikes leidub hulgaliselt turbaalasid. Kõige ajakohasema soode inventuuri kohaselt katavad turbaalad umbes 22,3% Eesti riigi territooriumist. See number aga ei peegelda kogu tõde, sest tuleb nentida, et enamus olemasolevatest turbaaladest on hääbumas. Tegelikkuses katab vaid 5,2% Eestimaa pindalast sood, mis loetakse aktiivse turbakasvuga aladeks. Ülejäänud turbaalasid võib seega lugeda pigem süsinikku vabastavateks kui seda siduvaks. Lisaks sellele tuleb ära märkida, et võrreldes eelmise sajandi keskpaigaga on soode kogupindala Eestis vähenenud peaaegu 2,8 korda, osutades drastilistele muutustele meie maastikes. Põhjused selliste muutuste taga on suures osas sarnased muu maailmaga, aga Eesti puhul paistab silma veel üks turbaalasid mõjutav tegur.

Nimelt on eesti turbaalad vähenenud ka maavarade kaevandamistegevuse tõttu. Antud mõjutused on kõige nähtavamad Kirde-Eestis, kus asub riigi kõige olulisem tööstusharu – põlevkivitööstus. Kõige silmapaistvamalt on turbaalade pindala vähenenud põlevkivi pealmaakaevandamise tõttu, kus kunagiste soode asemele on tekkinud karjäärid. Samas ammutatakse põlevkivi antud piirkonnas ka allmaakaevandustest, mille tegevusmõju avaldub eelkõige veetasemete alanemises regionaalsetes põhjaveekihtides. Kuigi allmaakaevandamise mõju soodele pole otseseselt tajutav, on turbalasundist allpool lasuvate veekihtide suuremahuline kuivendamine tekitanud arutelu, kas ja kui palju on sood antud kuivendusmõjutuste eest kaitstud. Kogu arutelu tuleneb peamiselt sellest, et kuigi enamuse piirkonnas asuvatest soodest võib liigitada rabade hulka, mis on sademeveetoitelised, on nad siiski mingil määral säilitanud oma seotuse allpool lasuvate põhjaveekihtidega.

Antud küsimustele lahenduse leidmiseks ning õigete looduskaitseliste otsuste tegemiseks tuleb eelkõige mõista soode hüdroloogiat – kuidas vesi erinevates turbakihtides liigub ja kuidas toimub veevahetus turba all lasuvate põhjaveekihtidega. Sellest tulenevalt on käesoleva doktoritöö põhieesmärkideks: (I) tõendada turbalasundi aluse kuivenduse mõju olemasolu ja uurida vee liikumist Kirde-Eestis asuva Selisoo raba näitel, mis asub aktiivse põlevkivi allmaakaevanduse vahetus läheduses ning (II) saada uusi andmeid soode füüsiliste ja hüdrauliliste parameetrite kohta ning pakkuda välja uusi vahendeid ja meetodeid, mida saaks edaspidi kasutatada, et uurida pinna- ja põhjaveekihtide omavahelisi seoseid ning hinnata turbalasundi aluse kuivenduse mõju ka teiste piirkonnas asuvate soode puhul.

Käesoleva töö jaoks koguti andmeid Selisoole paigutatud kahe veetasemete mõõtetransekti abil, mis ulatuvad soo äärtest, kuivendatud soometsadest kuni kahe eristatava rabakupli keskosani raba lõuna- ja põhjaosas. Ehitatud seiretransektidega koguti andmeid

kõigist veekihtidest, mis jäävad kaevanduse põhja ning soo pealispinna vahele. Töö tulemused kinnitavad, et kaevandustegevus ning sellest põhjustatud põhjaveetasemete langus aluspõhjalistes veekihtides mõjutab veetasemeid pinnakattelises Kvaternaari veekihis ning ka turbas. Selgub, et kaevandatava põlevkivikihi ning soo alumise pinna vahele jäävad aluspõhjalised veepidemed ei ole piisavad, et vältida veetasemete alanemist mineraalsetetes turbalasundi all. Kuigi kaevandamistegevus ei toimu otseselt Selisoo all, ulatub alanduslehter kaevanduse kuival hoidmiseks väljapumbatava põhjavee suure mahu tõttu vahepealsetes veekihtides ka soo piiridesse. Veetaseme langus turbaalustes Kvaternaari setetes on statistiliselt täheldatav kõigis Selisoole paigaldatud seirepunktides. Turbasse rajatud seirepunktides pole veetaseme langus kogu soo lõikes aga läbiv. Andmetele põhinedes paistab välja veetasemete langus raba ümber olevates kuivendatud soometsades (endised madal- ja siirdesood) ning põhjapoolsel transektil ka rabanõlval. Rabakuplite keskosades pole seireperioodi jooksul olnud veetasemete langus turbas statistiliselt oluline. Nähtav veetasemete muutumise dünaamika ja seirepunktide andmete omavaheline erinevus toovad esile turba enda olulisuse vee liikumise piiramisel soo pealispinnalt all lasuvatesse kuivendatud Kvaternaari setetesse. Olulist rolli mängivad turba paksus, mis väheneb raba äärealade suunas, ning selle hüdraulilised omadused. Vee liikumist piiravad eeldatavasti just turbalasundi kõige alumised madalsoo- ja siirdesoo turba kihid, mis on rohkem lagunenud ning kompakteerunud. Olulist rolli mängib ka antud kihtide lateraalne pidevus, mida võivad kohati olla rikkunud paremini vett juhtivad pinnakatte struktuurid.

Selisoos nähtu kinnitab turbalasundi aluste veekihtide kuivendamise mõju soo ökosüsteemile, mistõttu on tähtis ka teiste põlevkivi kaevandamise piirkonna soode füüsikaliste ja hüdrauliliste omaduste uurimine. Turba filtratsioonikoefitsienti (K_s) uuriti antud töö käigus kohapealsete pealevalamiskatsete ning BAT permeameetri katsetega. Füüsikaliste omaduste kirjeldamiseks sondeeriti turbalasundit, kirjeldati turbasüdamikud ning võeti proovid laboratoorseteks analüüsideks. Madal- ja siirdesoo turvas, mis moodustavad turbalasundi kõige alumise osa, on üldiselt kõige halvemini vett juhtivad turbakihid. Seetõttu on just need kihid kõige olulisemad vee vertikaalse liikumise takistamisel soopinnalt turbalasundi all olevatesse setetesse. Kirjelduste, katsete ja analüüside tulemustest selgub, et füüsikalised parameetrid nagu lasumissügavus, kuivmahukaal, lagunemisaste von Posti skaalal ja humifitseeritus on negatiivselt korreleerunud turba filtratsioonikoefitsiendiga. Kõigi mõõdetud füüsikaliste parameetrite ja filtratsioonikoefitsiendi vahel on statistiliselt oluline korrelatsioon. Nähtavate korrelatsioonide alusel koostati antud doktoritöö raames kaks mitmeparameetrilist statistilist mudelit, mis ennustaksid K_s väärtust nimetatud füüsikaliste parameetrite alusel. Lisaks eelnevalt mainitud arvtunnustele lisati mudelitesse ka soo arengufaasi iseloomustav nominaaltunnus. Mõlemad koostatud mudelid, millest üks kasutab turba lagunemisastme kirjeldamiseks von Posti väärtust ja teine humifikatsiooni, suudavad üsna hästi ennustada turba K_s väärtust. Lisaks näitasid mudelite tulemused, et kogutud andmestikul on asukohapõhine sõltuvus. Selline sõltuvus tuleneb ennekõike turbalasundi paksuse erinevusest asukohtade vahel ning lasundisisesest suurest heterogeensusest.

Samas tuleb nentida, et pealevalamis- ja permeameetri katsed ei suuda väga täpselt iseloomustada vee voolamist vertikaalsihis, mis on tähtis uurimaks just turbaalust kuivendusmõju soodele. Kõige tavalisemad meetodid vertikaalse filtratsioonikoefitsiendi (K_v) iseloomustamiseks eeldavad looduslikul kujul rikkumata turbaproovide võtmist ja laboratoorseid katseid. Esinduslike proovide saamine kogu turbalasundi lõikes võib aga osutuda väga keeruliseks, eriti just sügavamal olevatest kihtidest. Seetõttu tuleks eelistada kohapealseid katseid. Käesolevas doktoritöös pakutakse välja meetod K_v iseloomustamiseks,

mida pole varasemalt turba puhul kasutatud. Selle meetodi võlu peitub tema passiivses olemuses. K_v väärtus saadakse turbas samaaegselt erineval sügavusel mõõdetud vee hüdrauliliste survete ning õhurõhu seireandmetest. Nende andmete kaudu on võimalik arvutada turba vertikaalset piesojuhtivust (D_v) kahe erinevale sügavusele asetatud rõhusensori vahel, vaadeldes õhurõhu surveimpulsside amplituudide vähenemist ning hilinemist sügavuti aja jooksul. Teades turba eriveemahutavust (S_s), mis antud töös on iseloomustatud laboratoorselt mõõdetud kokkusurutavuse kaudu, on võimalik saadud D_v kaudu arvutada turba vertikaalne filtratsioonikoefitsient. Doktoritöö tulemused näitavad, et antud metoodika annab loogilisi ning võrreldavaid K_v tulemusi võrreldes teiste protseduuridega saadud väärtustega. Ennekõike sobib antud meetod just turbalasundi alumiste, rohkem lagunenud ja kompakteerunud turbakihtide K_v iseloomustamiseks. Vähem lagunenud ning pinnalähedasema rabaturba iseloomustamiseks võib antud meetod samuti sobida, kuid seda tuleks tulevikus veel täiendavalt uurida.

Käesolevas doktoritöös esitletud tulemused, andmed ja meetodid pakuvad annavad väärtuslikku informatsiooni Kirde-Eesti piirkonna rabade hüdroloogia kohta ning annavad ülevaate turbalasundi aluse kuivenduse potentsiaalsest mõjust soodele. Koostatud mudelid ja esitletud metoodika on praktilised ja olulised turbaalade edasisteks uuringuteks ning aitavad luua hüdroloogilisi ja hüdrogeoloogilisi mudeleid täpsemateks uuringuteks ja kuivenduse mõju hindamiseks.

ACKNOWLEDGEMENTS

I would like to thank my supervisors, Argo and Marko, for offering me the possibility of a PhD position and, of course, for including me in different projects, which have provided me with a lot of experience in the field. I guess without the awesome and friendly collective from the Department of Geology, this journey would have been much harder, so I am very grateful to them. Furthermore, I would like to acknowledge the Environmental Investment Centre for providing financial support (project 14533) which was used to collect data for this thesis.

I would also like to thank my family, who have supported me throughout my university years. Special thanks to my mom, without whom I guess I would not be a geologist right now, but also for inspiring me to pursue higher education from a very young age.

Lastly, my deepest gratitude goes to my wife, Marite, who has always stood beside me and offered her support, and willfully waited for me to conclude this endeavor.

PUBLICATIONS

CURRICULUM VITAE

Name: Raul Paat
Date of birth: 28.06.1993
Address: Department of Geology, University of Tartu,
Ravila 14A, 50411 Tartu, Estonia
Contact: +372 5622 2970
E-mail. raul.paat@ut.ee

Education

2018–…	University of Tartu, Department of Geology, PhD student in geology
2015–2018	University of Tartu, MSc in geology
2012–2015	University of Tartu, BSc in geology
2000–2012	Antsla Gymnasium

Professional employment

2020–…	Specialist, University of Tartu, Department of Geology
2018–2020	Specialist in Hydrogeology, University of Tartu, Department of Geology

Field of research:
Hydrogeology, hydrology, applied geology

Publications

Paat, R., Kohv, M., & Jõeleht, A. (2022). Saturated hydraulic conductivity of boreal peat and its relationships with peat properties and sampling depth. Hydrological Processes, 36(2), 1–12. https://doi.org/10.1002/hyp.14487

Kohv, M., **Paat, R**., Lõhmus, A., & Jõeleht, A. (2023). Underground mining magnifies drought impacts in an adjacent protected raised bog. Ecohydrology, 16(8). https://doi.org/10.1002/eco.2594

Paat, R., Jõeleht, A., Sarap, G. S., Kohv, M. (2024). Determining peat's vertical hydraulic diffusivity and hydraulic conductivity from naturally occurring hydraulic pressure fluctuations measured at various depths. Hydrological Processes, 38(7), 1–14. https://doi.org/10.1002/hyp.15236

ELULOOKIRJELDUS

Nimi: Raul Paat
Sünniaeg: 28.06.1993
Aadress: Geoloogia osakond, Tartu Ülikool,
Ravila 14A, 50411 Tartu, Estonia
Kontakt: +372 5622 2970
E-post: raul.paat@ut.ee

Haridus

2018–…	Tartu Ülikool, Geoloogia osakond, doktorantuur
2015–2018	Tartu Ülikool, MSc geoloogias
2012–2015	Tartu Ülikool, BSc geoloogias
2000–2012	Antsla Gümnaasium

Teenistuskäik

2020–…	Spetsialist, Tartu Ülikool, Geoloogia osakond
2018–2020	Hüdrogeoloogia spetsialist, Tartu Ülikool, Geoloogia osakond

Teadustöö põhisuunad:
Hüdrogeoloogia, hüdroloogia, rakendusgeoloogia

Publikatsioonid

Paat, R., Kohv, M., & Jõeleht, A. (2022). Saturated hydraulic conductivity of boreal peat and its relationships with peat properties and sampling depth. Hydrological Processes, 36(2), 1–12. https://doi.org/10.1002/hyp.14487

Kohv, M., **Paat, R**., Lõhmus, A., & Jõeleht, A. (2023). Underground mining magnifies drought impacts in an adjacent protected raised bog. Ecohydrology, 16(8). https://doi.org/10.1002/eco.2594

Paat, R., Jõeleht, A., Sarap, G. S., Kohv, M. (2024). Determining peat's vertical hydraulic diffusivity and hydraulic conductivity from naturally occurring hydraulic pressure fluctuations measured at various depths. Hydrological Processes, 38(7), 1–14. https://doi.org/10.1002/hyp.15236

DISSERTATIONES GEOLOGICAE UNIVERSITATIS TARTUENSIS

1. **Пээп Мянник.** Конодонты в верхнеордовикских и нижнесилурийских отложениях Эстонии. Тарту, 1992, 355 с.
2. **Elvi Tavast.** Fennoskandia kilbi lõunanõlva ja sellega piirnevate alade aluspõhja reljeef. Tartu, 1992, 357 lk.
3. **Kaarel Orviku.** Characterisation and evolution of Estonian seashores. Tartu, 1992, 19 p.
4. **Анатолий Молодьков.** ЭПР-анализ скелетного вещества моллюсков в хроностратиграфических исследованиях позднего кайнозоя. Тарту, 1992, 33 с.
5. **Jaan Lutt.** Late- and postglacial deposits on the Estonian shelf. Tartu, 1993, 31 p.
6. **Reet Karukäpp.** Gotiglatsiaalne morfogenees Skandinaavia mandriliustiku kagusektoris. Tartu, 1997, 181 p.
7. **Argo Jõeleht.** Geothermal studies of the Precambrian basement and Phanerozoic sedimentary cover in Estonia and Finland. Tartu, 1998, 125 p.
8. **Jüri Nemliher.** Mineralogy of Phanerozoic skeletal and sedimentary apatites: an XRD study. Tartu, 1999, 134 p.
9. **Kalle Kirsimäe.** Clay mineral diagenesis on the Lower Cambrian "Blue Clay" in the northern part of the Baltic Paleobasin. Tartu, 1999, 113 p.
10. **Jüri Plado.** Gravity and magnetic signatures of meteorite impact structures. Tartu, 2000, 87 p.
11. **Olev Vinn.** Morphogenesis and phylogenetic relationships of Clitambonitidines, Ordovician Brachiopods. Tartu, 2001, 127 p.
12. **Leho Ainsaar.** The middle Caradoc facies and faunal turnover in the late Ordovician Baltoscandian palaeobasin: sedimentological and carbon isotope aspects. Tartu, 2001, 109 p.
13. **Oive Tinn.** Early Ostracode evolution and Palaeoenvironmental application in the Ordovician of Baltoscandia. Tartu, 2002, 145 p.
14. **Maris Rattas.** Subglacial environments in the formation of drumlins — The case of the Saadjärve Drumlin Field, Estonia. Tartu, 2004, 117 p.
15. **Ene Kadastik.** Upper-Pleistocene stratigraphy and deglaciation history in northwestern Estonia. Tartu, 2004, 129 p.
16. **Helje Pärnaste.** Early Ordovician trilobites of suborder Cheirurina in Estonia and NW Russia: systematics, evolution and distribution. Tartu, 2004, 138 p.
17. **Mari-Ann Mõtus.** Silurian (Llandovery-Wenlock) tabulate corals of Baltoscandia: taxonomy, palaeoecology, distribution. Tartu, 2005, 167 p.
18. **Alar Rosentau**. Development of proglacial lakes in Estonia. Tartu, 2006, 114 p.
19. **Evelin Verš.** Development of impact-induced hydrothermal system at Kärdla impact structure. Tartu, 2006, 96 p.

20. **Sigitas Radzevičius.** The genus *Pristiograptus* in wenlock of East Baltic and the Holy Cross Mountains. Tartu, 2007, 133 p.
21. **Andres Marandi.** Natural chemical composition of groundwater as a basis for groundwater management in the Cambrian-Vendian aquifer system in Estonia. Tartu, 2007, 116 p.
22. **Eve Niinemets.** Vegetation and land-use history of the Haanja Heights (SE-Estonia) during the holocene. Tartu, 2008, 146 p.
23. **Kalle-Mart Suuroja.** Geology and lithology of the early palaeozoic marine impact stuctures Kärdla and Neugrund (Estonia). Tartu, 2008, 234 p.
24. **Rutt Hints.** Early diagenesis of Ordovician and Silurian Bentonites in the Northern Baltic Palaeobasin. Tartu, 2009, 90 p.
25. **Peeter Somelar.** Illitization of K-bentonites in the Baltic Basin. Tartu, 2009, 118 p.
26. **Ulla Preeden.** Remagnetizations in sedimentary rocks of Estonia and shear and fault zone rocks of southern Finland. Tartu, 2009, 121 p.
27. **Kati Tänavsuu-Milkeviciene.** Transgressive to regressive turnaround in the Middle Devonian Baltic Basin. Tartu, 2009, 106 p.
28. **Valle Raidla.** Chemical and isotope evolution of groundwater in the Cambrian-Vendian aquifer system in Estonia. Tartu, 2010, 134 p.
29. **Kadri Sohar.** Quaternary ostracods from Estonia and their application in palaeoenvironmental reconstruction. Tartu, 2010, 140 p.
30. **Kristjan Urtson.** Stepwise melt transport and accumulation: analogue and numerical modelling approach. Tartu, 2011, 83 p.
31. **Marko Kohv.** Landslides in clayey soils of western Estonia. Tartu, 2011, 116 p.
32. **Nele Muttik.** Post-impact alteration of impactites: Ries crater, Germany. Tartu, 2011, 78 p.
33. **Annette Sedman.** Strength and self-cementing properties of oil shale retorting wastes. Tartu, 2013, 82 p.
34. **Arkady Tsyrulnikov.** Complex seismo-acoustic and lithological study of the Lateglacial and postglacial sediments northern Gulf of Riga, eastern branch of the central Baltic Sea. Tartu, 2013, 102 p.
35. **Marge Uppin.** Geological sources and hydrochemistry of fluoride and boron in Silurian-Ordovician aquifer system. Tartu, 2013, 86 p.
36. **Peeter Talviste**. Temporal changes in weak natural and artificial soils – influence on geotechnical characteristics. Tartu, 2014, 204 p.
37. **Katrin Lasberg.** Chronology of the Weichselian Glaciation in the south-eastern sector of the Scandinavian Ice Sheet. Tartu, 2014, 100 p.
38. **Sirle Liivamägi.** Neoproterozoic Baltic paleosol: geology and paleoenvironmental interpretation. Tartu, 2015, 94 p.
39. **Lauri Joosu.** Petrography and the rare earth element composition of apatite in 2 Ga Onega and Pechenga basins, Russia: the environmental settings for phosphogenesis. Tartu, 2015, 139 p.
40. **Liisa Lang.** Baculate shell structure in Early Palaeozoic linguliform brachiopods. Tartu, 2015, 114 p.

41. **Päärn Paiste.** Geopolymeric potential of the Estonian oil shale processing waste. Tartu, 2017, 125 p.
42. **Mikk Gaškov.** Stable isotope and fluid inclusion evidence of multistage fluidal activity in Baltic paleobasin: Silurian carbonate sequence in Kalana, Estonia. Tartu, 2017, 104 p.
43. **Viirika Mastik.** Silurian noncalcified macroscopic algal fossils from the Kalana *Lagerstätte*, Estonia. Tartu, 2018, 91 p.
44. **Kairi Põldsaar.** Soft-sediment deformation and gravity flow structures in the Lower Palaeozoic successions of the Baltic Basin. Tartu, 2019, 105 p.
45. **Timmu Kreitsmann.** Application of carbon isotope and rare earth elements as recorders of environmental conditions in the aftermath of the Paleoproterozoic Lomagundi-Jatuli Event. Tartu, 2020, 163 p.
46. **Triine Nirgi.** Holocene relative shore-level changes and geoarchaeology of the prehistoric sites in western Estonia. Tartu, 2020, 161 p.
47. **Kristjan Leben.** Long-term diagenetic transformation and carbon sequestration potential of Ca-rich oil shale ash waste deposit sediments. Tartu, 2021, 117 p.
48. **Karin Truuver.** Ostracod associations of the ordovician–silurian boundary interval in baltoscandia. Tartu, 2021, 132 p.
49. **Kaarel Lumiste.** Phosphogenesis and REE+Y diagenesis of Recent and Paleozoic phosphorites. Tartu, 2021, 174 p.
50. **Sigrid Soomer.** Palaeoweathering record of the Archaean–Proterozoic transition in the Imandra–Varzuga Greenstone Belt, north-western Russia. Tartu, 2022, 114 p.
51. **Ivo Sibul.** Ground-penetrating radar in Estonia: from fieldwork to open data reuse. Tartu, 2023, 143 p.
52. **Tõnn Paiste.** Early evolution of the genus *Amorphognathus* and updated Sandbian (Upper Ordovician) conodont biostratigraphy in Baltoscandia. Tartu, 2023, 145 p.
53. **Sylvester Ikenna Ofili.** Geochemistry and depositional environments of two black shale formations: the Baltoscandian Cambrian-Ordovician Alum Shale and the Cretaceous Lokpanta Oil Shale. Tartu, 2024, 106 p.